# Characterization of a real-time tracer for isoprene epoxydiols-derived secondary organic aerosol (IEPOX-SOA) from aerosol mass spectrometer measurements

W. W. Hu, P. Campuzano-Jost, B. B Palm, D A Day, A M Ortega, P L Hayes, J. E Krechmer, Q. Chen, M. Kuwata, Y Liu, et al.

Atmos. Chem. Phys., 15, 11807–11833, 2015
www.atmos-chem-phys.net/15/11807/2015/
doi:10.5194/acp-15-11807-2015


Atmospheric Chemistry and Physics Open Access EGU

# Characterization of a real-time tracer for isoprene epoxydiols-derived secondary organic aerosol (IEPOX-SOA) from aerosol mass spectrometer measurements

**W. W. Hu[1,2], P. Campuzano-Jost[1,2], B. B. Palm[1,2], D. A. Day[1,2], A. M. Ortega[1,3], P. L. Hayes[1,2,a], J. E. Krechmer[1,2], Q. Chen[4,5], M. Kuwata[4,6], Y. J. Liu[4], S. S. de Sá[4], K. McKinney[4], S. T. Martin[4], M. Hu[5], S. H. Budisulistiorini[7], M. Riva[7], J. D. Surratt[7], J. M. St. Clair[8,b,c], G. Isaacman-Van Wertz[9], L. D. Yee[9], A. H. Goldstein[9,10], S. Carbone[11], J. Brito[11], P. Artaxo[11], J. A. de Gouw[1,2,12], A. Koss[2,12], A. Wisthaler[13,14], T. Mikoviny[13], T. Karl[15], L. Kaser[14,16], W. Jud[14], A. Hansel[14], K. S. Docherty[17], M. L. Alexander[18], N. H. Robinson[19,d], H. Coe[19], J. D. Allan[19,20], M. R. Canagaratna[21], F. Paulot[22,23], and J. L. Jimenez[1,2]**

[1]Cooperative Institute for Research in Environmental Sciences, University of Colorado, Boulder, CO, USA
[2]Department of Chemistry and Biochemistry, University of Colorado, Boulder, CO, USA
[3]Department of Atmospheric and Oceanic Sciences, University of Colorado, Boulder, CO, USA
[4]School of Engineering and Applied Sciences and Department of Earth and Planetary Sciences, Harvard University, Cambridge, MA, USA
[5]State Key Joint Laboratory of Environmental Simulation and Pollution Control, College of Environmental Sciences and Engineering, Peking University, Beijing, China
[6]Earth Observatory of Singapore, Nanyang Technological University, Singapore
[7]Department of Environmental Sciences and Engineering, Gillings School of Global Public Health, The University of North Carolina at Chapel Hill, Chapel Hill, NC, USA
[8]Division of Geological and Planetary Sciences, California Institute of Technology, Pasadena, CA, USA
[9]Department of Environmental Science, Policy, and Management, University of California, Berkeley, CA, USA
[10]Department of Civil and Environmental Engineering, University of California, Berkeley, CA, USA
[11]Department of Applied Physics, University of Sao Paulo, Sao Paulo, Brazil
[12]NOAA Earth System Research Laboratory, Boulder, CO, USA
[13]Department of Chemistry, University of Oslo, Oslo, Norway
[14]Institute for Ion Physics and Applied Physics, University of Innsbruck, Innsbruck, Austria
[15]Institute of Atmospheric and Cryospheric Sciences, University of Innsbruck, Innsbruck, Austria
[16]Atmospheric Chemistry Division (ACD), National Center for Atmospheric Research, Boulder, CO, USA
[17]Alion Science and Technology, Research Triangle Park, NC, USA
[18]Environmental Molecular Sciences Laboratory, Pacific Northwest National Laboratory, Richland, WA, USA
[19]School of Earth, Atmospheric and Environmental Sciences, University of Manchester, Oxford Road, Manchester, UK
[20]National Centre for Atmospheric Science, University of Manchester, Oxford Road, Manchester, UK
[21]Aerodyne Research, Inc., Billerica, MA, USA
[22]NOAA Geophysical Fluid Dynamics Laboratory, Princeton, NJ, USA
[23]Program in Atmospheric and Oceanic Sciences, Princeton University, Princeton, NJ, USA
[a]now at: Department of Chemistry, Université de Montréal, Montréal, QC, Canada
[b]now at: Atmospheric Chemistry and Dynamics Laboratory, NASA Goddard Space Flight Center, Greenbelt, MD, USA
[c]now at: Joint Center for Earth Systems Technology, University of Maryland Baltimore County, Baltimore, MD, USA
[d]now at: Met Office, Exeter, UK

*Correspondence to:* J. L. Jimenez (jose.jimenez@colorado.edu)

Received: 3 March 2015 – Published in Atmos. Chem. Phys. Discuss.: 16 April 2015
Revised: 16 August 2015 – Accepted: 25 September 2015 – Published: 23 October 2015

**Published by Copernicus Publications on behalf of the European Geosciences Union.**

**Abstract.** Substantial amounts of secondary organic aerosol (SOA) can be formed from isoprene epoxydiols (IEPOX), which are oxidation products of isoprene mainly under low-NO conditions. Total IEPOX-SOA, which may include SOA formed from other parallel isoprene oxidation pathways, was quantified by applying positive matrix factorization (PMF) to aerosol mass spectrometer (AMS) measurements. The IEPOX-SOA fractions of organic aerosol (OA) in multiple field studies across several continents are summarized here and show consistent patterns with the concentration of gas-phase IEPOX simulated by the GEOS-Chem chemical transport model. During the Southern Oxidant and Aerosol Study (SOAS), 78 % of PMF-resolved IEPOX-SOA is accounted by the measured IEPOX-SOA molecular tracers (2-methyltetrols, C5-Triols, and IEPOX-derived organosulfate and its dimers), making it the highest level of molecular identification of an ambient SOA component to our knowledge. An enhanced signal at $C_5H_6O^+$ ($m/z$ 82) is found in PMF-resolved IEPOX-SOA spectra. To investigate the suitability of this ion as a tracer for IEPOX-SOA, we examine $f_{C_5H_6O}$ ($f_{C_5H_6O} = C_5H_6O^+/OA$) across multiple field, chamber, and source data sets. A background of $\sim 1.7 \pm 0.1$ ‰ (‰ = parts per thousand) is observed in studies strongly influenced by urban, biomass-burning, and other anthropogenic primary organic aerosol (POA). Higher background values of $3.1 \pm 0.6$ ‰ are found in studies strongly influenced by monoterpene emissions. The average laboratory monoterpene SOA value ($5.5 \pm 2.0$ ‰) is 4 times lower than the average for IEPOX-SOA ($22 \pm 7$ ‰), which leaves some room to separate both contributions to OA. Locations strongly influenced by isoprene emissions under low-NO levels had higher $f_{C_5H_6O}$ ($\sim 6.5 \pm 2.2$ ‰ on average) than other sites, consistent with the expected IEPOX-SOA formation in those studies. $f_{C_5H_6O}$ in IEPOX-SOA is always elevated (12–40 ‰) but varies substantially between locations, which is shown to reflect large variations in its detailed molecular composition. The low $f_{C_5H_6O}$ (< 3 ‰) reported in non-IEPOX-derived isoprene-SOA from chamber studies indicates that this tracer ion is specifically enhanced from IEPOX-SOA, and is not a tracer for all SOA from isoprene. We introduce a graphical diagnostic to study the presence and aging of IEPOX-SOA as a *triangle plot* of $f_{CO_2}$ vs. $f_{C_5H_6O}$. Finally, we develop a simplified method to estimate ambient IEPOX-SOA mass concentrations, which is shown to perform well compared to the full PMF method. The uncertainty of the tracer method is up to a factor of $\sim 2$, if the $f_{C_5H_6O}$ of the local IEPOX-SOA is not available. When only unit mass-resolution data are available, as with the aerosol chemical speciation monitor (ACSM), all methods may perform less well because of increased interferences from other ions at $m/z$ 82. This study clarifies the strengths and limitations of the different AMS methods for detection of IEPOX-SOA and will enable improved characterization of this OA component.

## 1 Introduction

Isoprene (2-methyl-1,3-butadiene, $C_5H_8$) emitted by vegetation is the most abundant non-methane hydrocarbon emitted to the Earth's atmosphere ($\sim$ 440–600 TgC year$^{-1}$) (Guenther et al., 2012). It is estimated to contribute substantially to the global secondary organic aerosol (SOA) budget (Paulot et al., 2009b; Guenther et al., 2012). Higher SOA yields from isoprene are observed under low-$NO_x$ conditions (Surratt et al., 2010). Under low-NO conditions, i.e. when a substantial fraction of the peroxy radicals do not react with NO, gas-phase isoprene epoxydiols (IEPOX) are produced with high yield through a $HO_x$-mediated mechanism (Paulot et al., 2009b). Note that some IEPOX can also be formed from isoprene in a high-NO region via oxidation of the product 4-hydroxy-3-nitroxy isoprene (Jacobs et al., 2014); however, this pathway is thought to be much smaller than the low-NO pathway. Subsequently, IEPOX can be taken up by acidic aerosols (Gaston et al., 2014), where IEPOX-SOA can be formed through acid-catalyzed oxirane ring opening of IEPOX (Cole-Filipiak et al., 2010; Eddingsaas et al., 2010; Lin et al., 2012; Nguyen et al., 2014), which is thought to be the main pathway to form IEPOX-SOA (Surratt et al., 2010; Pye et al., 2013; Worton et al., 2013). Although the complete molecular composition of IEPOX-SOA has not been elucidated, several molecular species that are part of IEPOX-SOA have been identified through gas chromatography/mass spectrometry (GC/MS), liquid chromatography/mass spectrometry (LC/MS), and particle analysis by laser mass spectrometry (PALMS). They include 2-methyltetrols (and oligomers that contain them) (Surratt et al., 2010; Lin et al., 2014), $C_5$-alkene triols (Wang et al., 2005), 3-methyltetrahydrofuran-3,4-diols (Lin et al., 2012), and an IEPOX-organosulfate (Froyd et al., 2010; Liao et al., 2014). These molecular species account for a variable fraction of the IEPOX-SOA reported, e.g., 8 % in a chamber study (Lin et al., 2012) or 26 % in a field study at Look Rock, TN (Budisulistiorini et al., 2015). An estimate of total IEPOX-SOA can also be derived from an IEPOX-SOA molecular tracer(s) via multiplying the tracer concentration by the total IEPOX-SOA to tracer ratio. However, that method is hindered by the limited information on these molecular tracers and the reported variability of IEPOX-SOA to tracer ratios. IEPOX-SOA may include SOA formed from other parallel isoprene low-NO oxidation pathways (Liu et al., 2014; Krechmer et al., 2015). In addition, the IEPOX-SOA molecular tracers are typically measured with slow time resolution (12/24 h).

Multiple field studies, supported by chamber studies, have shown that the total amount of IEPOX-SOA can be obtained

by factor analysis of organic spectra from an aerosol mass spectrometer (AMS) or the aerosol chemical speciation monitor (ACSM) (Robinson et al., 2011; Lin et al., 2012; Budisulistiorini et al., 2013; Nguyen et al., 2014). Robinson et al. (2011) first reported an SOA factor with pronounced $f_{82}$ (i.e., $m/z$ 82/OA) in the mass spectra acquired above a forest with high isoprene emissions in Borneo, and hypothesized that the elevated $f_{82}$ may have arisen from methylfuran ($C_5H_6O$), consistent with $C_5H_6O^+$ being the major ion at $m/z$ 82 in isoprene-influenced areas. Lin et al. (2012) demonstrated that the 3-MeTHF-3,4-diols associated with IEPOX-SOA result in enhanced $f_{82}$ in AMS spectra, presumably through the formation of methylfuran-like structures during thermal desorption. Electron-impact ionization of aerosols formed by atomizing a solution containing IEPOX ($C_5H_{10}O_3$) can also yield $C_5H_6O^+$ signals in an AMS via two dehydration reactions (Lin et al., 2012). However, because gas-phase IEPOX has high volatility, non-reactive gas-to-particle partitioning of IEPOX into organic aerosol (OA) is negligible under typical ambient concentrations in forest areas (1–10 µg m$^{-3}$) (Worton et al., 2013).

IEPOX-SOA was estimated to account for 33 % of ambient OA in summertime Atlanta from PMF analysis of ACSM spectra. The source apportionment result was supported by the pronounced $f_{82}$ peak in the factor spectrum and good temporal correlation of the factor with sulfate and 2-methyltetrols (Budisulistiorini et al., 2013). Sulfate is often strongly correlated with the acidity of an aerosol, and might also play a direct role in the chemistry, e.g. via direct reaction or nucleophilic effects (Surratt et al., 2007; Liao et al., 2014; Xu et al., 2014). While discussing the results of a recent aircraft campaign from Brazil, Allan et al. (2014) also used $f_{82}$ as a tracer for IEPOX-SOA.

If $f_{82}$ in AMS spectra (and/or $f_{C_5H_6O}$ in HR-AMS spectra) is dominated by IEPOX-SOA, $f_{82}$ would be a convenient, high time resolution, and potentially quantitative tracer for IEPOX-SOA. Thus, it will be very useful for investigating the impacts of SOA formation from isoprene with AMS/ACSM measurements, which have become increasingly common in recent years including some continental-scale continuous networks (Fröhlich et al., 2015). However, no studies to date have systematically examined whether enhanced $f_{82}$ is unique to IEPOX chemistry or whether it could also be enhanced in other sources. Nor has the range of $f_{82}$ been determined for IEPOX-SOA. Questions also have been raised about the uniqueness of this tracer and potential contributions from monoterpene SOA (Anonymous Referee, 2014).

In this study, the IEPOX-SOA results reported in various field campaigns are summarized and compared to predicted gas-phase IEPOX concentrations from a global model to help confirm the robustness of the AMS identification of this type of SOA. We then investigate the usefulness and limitations of the IEPOX-SOA tracers $f_{C_5H_6O}$ (i.e., $C_5H_6O^+$/OA) and $f_{82}$ by combining AMS data from multiple field and laboratory studies including a new data set from the 2013 Southern Oxidant and Aerosol Study (SOAS). We compare the tracer levels in different OA sources (urban, biomass burning, and biogenic), characterizing the background levels and interferences on this tracer for both high-resolution (HR) and unit mass-resolution (UMR) data. We also provide a simplified method to rapidly estimate IEPOX-SOA from $f_{C_5H_6O}$ and $f_{82}$. While this method is no substitute for a detailed IEPOX-SOA identification via PMF, it is a simple method to estimate IEPOX-SOA concentrations (or its absence) in real time from AMS or ACSM measurements or under conditions in real time, or where PMF analysis is not possible or is difficult to perform.

## 2 Experimental

We classify the field data sets used in this study into three categories: (1) studies strongly influenced by urban and biomass-burning emissions: Los Angeles area, USA, and Beijing, China (urban); Changdao island, downwind of China, and Barcelona area, Spain (urban downwind); flight data from biomass-burning plumes and continental areas (NW and western, USA) in SEAC4RS and DC3 campaigns; and biomass-burning lab emissions (FLAME-3 study). (2) Studies strongly influenced by isoprene emissions, including a SE US forest site (SOAS campaign); Two pristine forest site and one forest site partially impacted by urban plumes in the Amazon rain forest (Brazil). The latter site is classified in this category because (i) high isoprene concentrations (e.g. 3 ppb in average peaks in the afternoon) were observed during the study; (ii) the impact of biogenic SOA formed during 1000 km where the air travels over the pristine forest upwind of Manaus; (iii) PMF results indicate an important impact of IEPOX-SOA at this site (de Sá et al., 2015); (iv) PTRMS results indicate a substantial concentration of the isoprene hydroperoxyde formed by low-NO chemistry, Borneo rain forest in Malaysia, and flight data from SE US flights from aircraft campaign (SEAC4RS). (3) Studies strongly influenced by monoterpene emissions in a pine forest in the Rocky Mountains and a European boreal forest. Locations and additional detailed information about these studies can be found in Fig. 1 and Table 1.

With the exception of SOAS, all of the campaigns included in this analysis have been previously described elsewhere (Table 1). The SOAS campaign took place in a forested area of the SE USA during June and July 2013 (Fig. 1) and has several ground sites. The new data set introduced below was acquired at the SEARCH supersite, Centreville (CTR), AL (32.95° N, 87.13° W). Some results from a different SOAS site (Look Rock, TN) are also discussed later (Budisulistiorini et al., 2015). Relatively high average isoprene and monoterpene concentrations of $3.3 \pm 2.4$ and $0.7 \pm 0.4$ ppb, respectively, were observed in SOAS-CTR by online GC/MS. Measurements of non-refractory aerosol components of submicron particles ($PM_1$) were made using

**Table 1.** Data sets used in this study[a]. Ranges or average plus standard deviation of $f_{C_5H_6O}$ (high resolution) and $f_{82}$ (unit mass resolution) in different studies are also included.

| Name of data sets | Time period | Site locations and descriptions | Campaign name | Ranges or average ± SD $f_{C_5H_6O}$ (‰) | Ranges or average ± SD $f_{82}$ (‰) | References |
|---|---|---|---|---|---|---|
| Studies strongly influenced by isoprene emissions under lower NO | | | | | | |
| SE US forest-CTR site | Jun–Jul 2013 | Centreville, AL, USA | SOAS | 6.2 ± 2.4 | 7.6 ± 2.2 | (1) |
| Pristine Amazon forest 2008, Brazil | Feb–Mar 2008 | Pristine rain forest site, TT34 | AMAZE-08 | 5.0 ± 2.3 | 7.9 ± 1.7 | (2) |
| Amazon forest downwind Manaus, Brazil | Feb–Mar 2014 | T3 site, near Manacapuru | GoAmazon2014/5 | 6.9 ± 1.6 | 7.1 ± 1.0 | (3) |
| Pristine Amazon forest 2014, Brazil | Aug–Dec 2014 | T0 site, ∼ 150 km northeast of Manaus | GoAmazon2014/5 | NA | 5.6 ± 1.7 | (4) |
| SE USA | Aug–Sep 2013 | Aircraft measurement | SEAC4RS | 4.3 ± 1.6 | NA | (5) |
| Borneo forest, Malaysia | Jun–Jul 2008 | Rain forest GAW station, Sabah, Malaysia | OP3 | 10 ± 0.3 | 12.4 ± 0.4 | (6) |
| Atlanta, USA | Aug–Sep 2011 | Urban JST site, Atlanta, Georgia, USA | NA | NA | 3.7 ± 1.9 | (7) |
| Atlanta (JST), USA | May 2012 | Urban JST site, Atlanta, Georgia, USA | NA | 3.3 ± 0.9 | NA | (8) |
| Atlanta (GT), USA | Aug 2012 | Urban Georgia Tech site, Georgia, USA | NA | 5.4 ± 1.9 | NA | (8) |
| Yorkville, USA | July 2012 | Rural sites, 80 km northwest of JST site, Georgia, USA | NA | 7.7 ± 2.2 | NA | (8) |
| Harrow, Canada | Jun–Jul 2007 | Harrow site, rural sites surrounded by farmland, Canada | BAQSMET | NA | NA | (9) |
| Bear Creek, Canada | Jun–Jul 2007 | Bear Creek site, wetlands area surrounded by farmland, Canada | BAQSMET | NA | NA | (9) |
| Studies strongly influenced by monoterpene emissions | | | | | | |
| Rocky mountain pine forest, CO, USA | Jul–Aug 2011 | Manitou Experimental Forest Observatory, CO, USA | BEACHON-RoMBAS | 3.7 ± 0.5 | 5.1 ± 0.5 | (10) |
| European Boreal forest, Finland | 2008–2009 | Hyytiälä site in Pine forest, Finland | EUCAARI campaign | 2.5 ± 0.1[b] | 4.8 ± 0.1[b] | (11) |
| Studies mixed-influenced by isoprene and monoterpene emissions | | | | | | |
| North American temperate, USA | Aug–Sep 2007 | Blodgett Forest Ameriflux Site, CA, USA | BEARPEX | 4.0 ± < 0.1[b] | 4.0 ± < 0.1[b] | (11) |
| Studies strongly influenced by urban emissions | | | | | | |
| Los Angeles area , CA, USA | May–Jun 2010 | Pasadena, USA | CalNex | 1.6 ± 0.2 | 3.6 ± 0.5 | (12) |
| Beijing, China | Nov–Dec 2010 | Peking University, in NW of Beijing city, China | NA | 1.5 ± 0.3 | 4.6 ± 0.7 | (13) |
| Changdao island, Downwind of China | Mar–Apr 2011 | Changdao island, China | CAPTAIN | 1.6 ± 0.2 | 3.8 ± 0.5 | (14) |
| Barcelona area, Spain | Feb–Mar 2009 | Montseny, Spain | DAURE | 1.6 ± 0.2 | 4.8 ± 0.9 | (15) |
| Studies of biomass-burning smokes | | | | | | |
| BB Chamber study | Sep–Oct 2009 | Missoula, MO, USA | FLAME-3 | 1.9 ± 0.6 | 5.9 ± 1.4 | (16) |
| Biomass-burning plumes | Aug–Sep 2013 | All over USA, aircraft measurement | SEAC4RS | 1.8 ± 0.5 | NA | (6) |
| Biomass-burning plumes | May–Jun 2011 | All over USA, aircraft measurement | DC-3 | 1.8 ± 0.4 | NA | (17) |
| Continental plumes | | | | | | |
| NW US | Aug–Sep 2013 | Aircraft measurement | SEAC4RS | 1.7 ± 0.3 | NA | (16) |
| Western USA | May–Jun 2011 | Aircraft measurement | DC-3 | 1.9 ± 0.6 | NA | (17) |
| OA from specific sources | | | | | | |
| IEPOX-SOA from ambient PMF factors and chamber studies. | | | | 22 ± 7 | 22 ± 7 | (18) |
| Isoprene-derived non-IEPOX SOA (reaction with OH under conditions of high NO or low NO without seed not favorable for the reactive uptake of IEPOX, reaction with $NO_3$ without seed) | | | | <3 | <3 | (19) |
| Monoterpene-derived SOA | | | | 5.5 ± 2.0 | 6.7 ± 2.0 | (20) |
| Other SOA (not from isoprene and mononterpene) | | | | 2.2 ± 0.9 | 6.1 ± 2.1 | (21) |
| Cooking | | | | 1.5 ± 0.8 | 8.2 ± 1.1 | (22) |
| Coal combustion | | | | 1.4–2.0 | NA | (23) |
| Vehicle emission | | | | 1.1 ± 0.6 | 5.1 ± 1.1 | (24) |
| Biomass burning | | | | 2.3 ± 0.7 | 4.3 ± 1.5 | (25) |
| Pure chemical species | | | | 0.7 ± 1.0 | 4.0 ± 5.5 | (26) |

[a] HR-ToF-AMS was used for all the campaigns except the Atlanta, USA, and Pristine Amazon forest 2014, Brazil, using ACSM. [b] Standard error. (1) This study, (2) Chen et al. (2015), (3) de Sá et al. (2015), (4) Carbone et al. (2015), (5) Liao et al. (2014), (6) Robinson et al. (2011), (7) Budisulistiorini et al. (2013), (8) Xu et al. (2014, 2015), (9) Slowik et al. (2011), (10) Ortega et al. (2014), (11) Robinson et al. (2011), (12) Hayes et al. (2013), (13) Hu et al. (2015), (14) Hu et al. (2013), (15) Minguillón et al. (2011), (16) Ortega et al. (2013), (17) Barth et al. (2015), (18) Chhabra et al. (2011), Robinson et al. (2011), Budisulistiorini et al. (2013), Chen et al. (2015), Liu et al. (2014), Kuwata et al. (2015), (19) Kroll et al. (2006), Ng et al. (2008), Krechmer et al. (2015), (20) Bahreini et al. (2005), Chen et al. (2015), Boyd et al. (2015), (21) Bahreini et al. (2005), Liggio et al. (2005), Chhabra et al. (2011), Loza et al. (2012), (22) Lanz et al. (2007), Mohr et al. (2009, 2012), He et al. (2010), Huang et al. (2010), Crippa et al. (2013), Hu et al. (2015), (23) Hu et al. (2013, 2015), (24) Canagaratna et al. (2004), Lanz et al. (2007), Sage et al. (2008), Aiken et al. (2009), Mohr et al. (2009, 2012), Chang et al. (2011), Docherty et al. (2011), Hersey et al. (2011), Ng et al. (2011b), Coggon et al. (2012), Saarikoski et al. (2012), Setyan et al. (2012), Crippa et al. (2013), (25) Schneider et al. (2006, 2011), Weimer et al. (2008), Aiken et al. (2009), He et al. (2010), Ng et al. (2011b), Mohr et al. (2012), Saarikoski et al. (2012), Crippa et al. (2013), Hu et al. (2013, 2015), (26) Alfarra (2004), Katrib et al. (2004), Phinney et al. (2006), Dzepina et al. (2007), Takegawa et al. (2007), Aiken et al. (2009), Li et al. (2011), and Schneider et al. (2011).

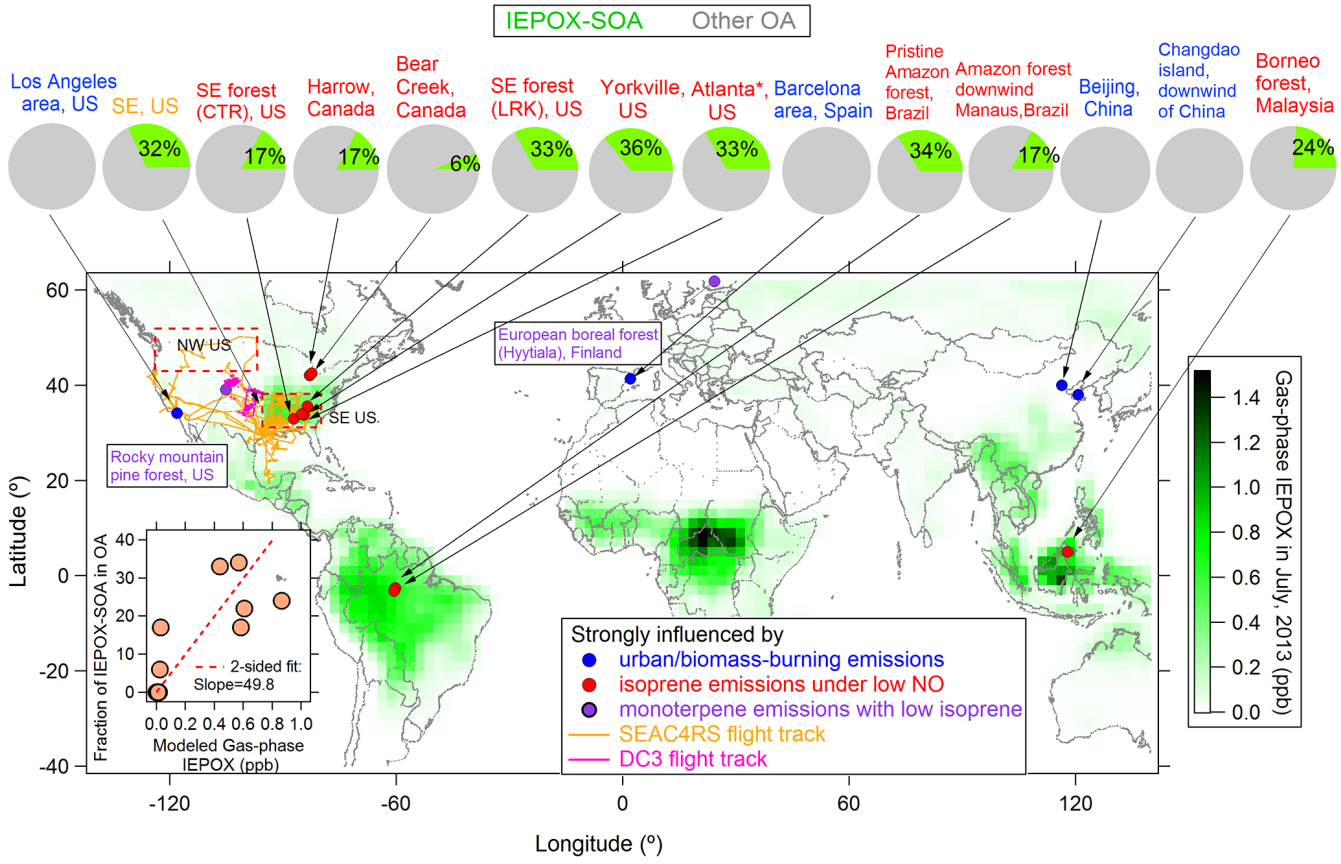


**Figure 1.** Locations of field campaigns used in this study. The IEPOX-SOA fractions of OA in different studies are shown in the pie charts on the top of graph. Site names are color coded with site types. Detailed information these studies can be found in Table 1. Note that the Atlanta pie chart was averaged by three urban data sets in Budisulistiorini et al. (2013) and Xu et al. (2015). The green background is color coded with modeled global gas-phase IEPOX concentrations for July 2013 from the GEOS-Chem model. The insert shows as scatter plot of observed average fraction of IEPOX-SOA in OA vs. GEOS-Chem modeled gas-phase IEPOX in various field campaigns.

an Aerodyne high-resolution time-of-flight aerosol mass spectrometer (HR-ToF-AMS; AMS hereafter) (DeCarlo et al., 2006). By applying positive matrix factorization (PMF) to the time series of organic mass spectra (Ulbrich et al., 2009), we separated contributions from IEPOX-SOA and other sources/components of OA. The AMS PMF results used here are very consistent with those from a separate AMS operated by another group at the same site (Xu et al., 2014). The global gas-phase IEPOX concentrations in 2013 were modeled at a resolution of $2 \times 2.5°$ as described in Nguyen et al. (2015). The gas-phase chemistry of isoprene in GEOS-Chem is based on Paulot et al. (2009a, b) as described by Mao et al. (2013).

In the following discussion, we denote the IEPOX-SOA factor from PMF as "IEPOX-SOA$_{PMF}$" and IEPOX-SOA from lab studies as "IEPOX-SOA$_{lab}$" for clarity. If we use "IEPOX-SOA" in the paper, it refers to a broad concept of IEPOX-SOA. We use a superscript to clarify the type of OA for which $f_{C_5H_6O}$ is being discussed: $f_{C_5H_6O}^{OA}$ refers to $f_{C_5H_6O}$ in total OA, $f_{C_5H_6O}^{IEPOX\text{-}SOA}$ to $f_{C_5H_6O}$ in IEPOX-SOA$_{PMF}$ or IEPOX-SOA$_{lab}$, $f_{C_5H_6O}^{MT\text{-}SOA}$ to the $f_{C_5H_6O}$ value in pure MT-SOA and $f_{C_5H_6O}^{OA\text{-}Bkg\text{-}UB}$, and $f_{C_5H_6O}^{OA\text{-}Bkg\text{-}MT}$ refer to background $f_{C_5H_6O}^{OA}$ from areas strongly influenced by urban+biomass-burning emissions and by monoterpene emissions, respectively. If we refer to $f_{C_5H_6O}$ in general, we will still use $f_{C_5H_6O}$. When we report the average $f_{C_5H_6O}^{OA}$ in each campaign, as shown in the Table 1, we used the average from the time series of $f_{C_5H_6O}^{OA}$ at their raw time resolution (seconds to minutes). During this process, we exclude points whose OA mass concentrations are below twice the detection limit of OA in AMS (typically $2 \times 0.26\,\mu g\,m^{-3} = 0.5\,\mu g\,m^{-3}$). When averaging $f_{C_5H_6O}^{OA}$ values across data sets, we counted each data set as one data point.

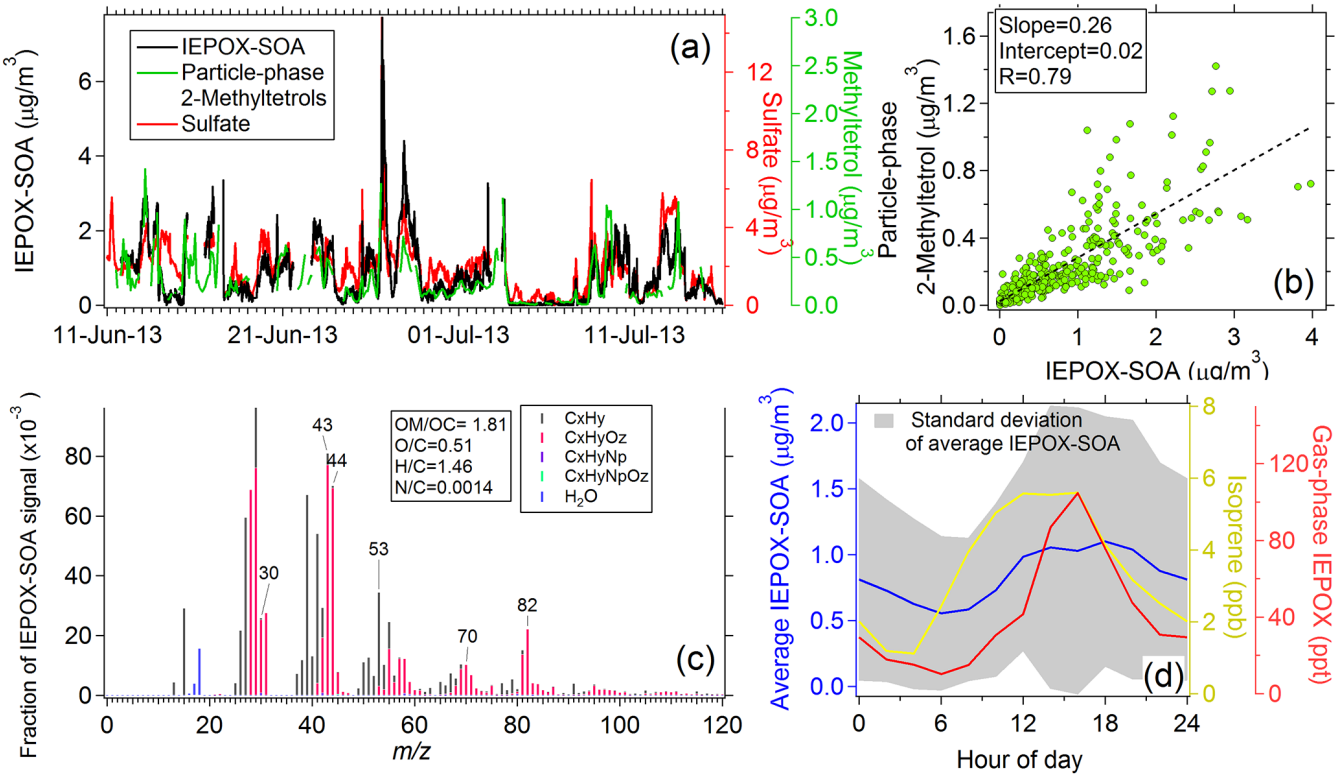


**Figure 2.** Results from the SOAS campaign in a SE US forested site. **(a)** Time series of IEPOX-SOA$_{PMF}$, sulfate, and particle-phase 2-methylterols (a key IEPOX uptake product) from on-line GC/MS; **(b)** Scatter plot between particle-phase 2-methylterols and IEPOX-SOA. **(c)** Mass spectrum of IEPOX-SOA; **(d)** Diurnal cycle of IEPOX-SOA, isoprene, and gas-phase IEPOX (the latter measured by $CF_3O^-$ CIMS).

## 3 Results and discussion

### 3.1 IEPOX-SOA in a SE US forest during SOAS, 2013

We use the SOAS-CTR field study (SE US-CTR) as an example for the determination of IEPOX-SOA from AMS data via PMF analysis. The time series and mass spectrum of this component are shown in Fig. 2. The IEPOX-SOA$_{PMF}$ mass concentration is the sum of mass concentrations of all the ions in the IEPOX-SOA$_{PMF}$ mass spectra. The "mass concentration" of an ion is used to represent the mass of the species whose detection resulted in the observed ion current of that ion, based on the properties of electron ionization (Jimenez et al., 2003). An uncertainty (standard deviation) of IEPOX-SOA$_{PMF}$ mass concentration of $\sim 9\,\%$ was estimated from 100 bootstrapping runs in PMF analysis (Ulbrich et al., 2009) (Fig. S1 in the Supplement). This uncertainty concerns only the PMF separation method. In practice the uncertainty in IEPOX-SOA$_{PMF}$ concentration is dominated by the larger uncertainty on the AMS concentrations arising from the collection efficiency and relative ionization efficiency (Middlebrook et al., 2012).

A strong correlation is found between AMS IEPOX-SOA$_{PMF}$ and 2-methyltetrols ($R = 0.79$) and sulfate ($R = 0.75$) as expected (Surratt et al., 2010; Lin et al., 2012; Nguyen et al., 2014; Xu et al., 2014). The diurnal variation of IEPOX-SOA$_{PMF}$ is also similar to gas-phase IEPOX and isoprene measured in SOAS-CTR. 2-Methyltetrols, measured online by GC-EI/MS with the SV-TAG instrument (Isaacman et al., 2014), comprise 26 % of IEPOX-SOA$_{PMF}$ in SOAS-CTR on average, as shown in Fig. 2b. A similar ratio (29 %) is found between 2-methyltetrols measured by offline analysis of filter samples using GC-EI/MS and LC/MS (Lin et al., 2014) and IEPOX-SOA$_{PMF}$. Other IEPOX-SOA tracers, such as C5-alkene triols, IEPOX-organosulfates, and dimers containing them, can also be measured by offline GC-EI/MS and LC/MS (Lin et al., 2014; Budisulistiorini et al., 2015), and they account for 28 and 24 % in total IEPOX-SOA$_{PMF}$ in SOAS ($R = 0.7$) (Fig. S2). The total IEPOX-SOA tracers measured in SOAS account for $\sim 78 \pm 42\,\%$ of the total IEPOX-SOA$_{PMF}$ mass concentration. The uncertainty of the fraction of IEPOX-SOA molecular tracers in IEPOX-SOA$_{PMF}$ in SOAS study (42%) is estimated by combining the overall uncertainty from IEPOX-SOA molecular tracer measurement (24 %), linear regression between tracer vs. IEPOX-SOA$_{PMF}$ (17 %, see Figs. 2b and S2), IEPOX-SOA$_{PMF}$ in PMF separation method (9 %) and the quantification of IEPOX-SOA$_{PMF}$ based on AMS calibration (30 %)

(Middlebrook et al., 2012). This is a remarkably high value compared to the tracer to total SOA ratios for other SOA systems (e.g., SOA from monoterpenes or aromatic hydrocarbons) (Lewandowski et al., 2013). A total tracers to IEPOX-SOA$_{PMF}$ ratio of 26 % was reported for the Look Rock site in SOAS (SOAS-LR) (Budisulistiorini et al., 2015). Thus, the measured total molecular tracer fraction in total IEPOX-SOA appears to be quite variable (a factor of 3) even if the same or similar techniques are used. Although the calibration methodology between different campaigns may result in some uncertainties, this value likely changes significantly between different times and locations, potentially due to changes in particle-phase reaction conditions such as sulfate and water concentrations, acidity, and the identity and concentrations of oligomerization partners.

IEPOX-SOA$_{PMF}$ accounts for 17 % of the total OA mass concentration at SOAS-CTR. This is shown in Fig. 1 along with the IEPOX-SOA$_{PMF}$ fraction from several previous studies (Robinson et al., 2011; Slowik et al., 2011; Budisulistiorini et al., 2013; Hayes et al., 2013; Hu et al., 2013; Chen et al., 2015; Hu et al., 2015). Figure 1 also shows the surface gas-phase IEPOX concentrations for July 2013 as simulated with GEOS-Chem. At all sites with at least $\sim$ 30 ppt predicted average IEPOX concentration, IEPOX-SOA$_{PMF}$ is identified in AMS data. IEPOX-SOA$_{PMF}$ accounts for 6–36 % of total OA in those studies, signifying the importance of IEPOX-SOA for regional and global OA budgets. No IEPOX-SOA$_{PMF}$ factor (i.e. below the PMF detection limit of $\sim$ 5 % of OA; Ulbrich et al., 2009) was found in areas strongly influenced by urban emissions where high-NO concentrations suppress the IEPOX pathway, even in the presence of substantial isoprene concentrations (e.g. Hayes et al., 2013). GEOS-Chem indeed predicts negligible modeled gas-phase IEPOX concentrations in those areas, where isoprene peroxy radicals are expected to react primarily with NO. Some IEPOX can also be formed via high-NO chemistry (Jacobs et al., 2014); however, this pathway is thought to be much smaller than the low-NO pathway, consistent with the lack of observation of IEPOX-SOA$_{PMF}$ in the polluted studies included here. The fraction of IEPOX-SOA$_{PMF}$ positively correlates with modeled gas-phase IEPOX, as shown in the inset of Fig. 1.

The mass spectrum of IEPOX-SOA during SOAS-CTR is similar to those from other studies as seen in Figs. S3–S4 (Robinson et al., 2011; Lin et al., 2012; Budisulistiorini et al., 2013; Chen et al., 2015; Nguyen et al., 2014; Xu et al., 2014), and also exhibits a prominent $C_5H_6O^+$ peak at $m/z$ 82. We investigated the correlation between the time series of IEPOX-SOA$_{PMF}$ and each ion in the OA spectra. The temporal variation of ion $C_5H_6O^+$ correlates best ($R = 0.96$) with IEPOX-SOA$_{PMF}$ among all measured OA ions (Table S1). This result suggests that $C_5H_6O^+$ ion may be the best ion tracer for IEPOX-SOA among all OA ions. $C_5H_5O^+$ ($m/z$ 81), $C_4H_5^+$ ($m/z$ 53), $C_4H_6O^+$ ($m/z$ 70), and $C_3H_7O_2^+$ ($m/z$ 75) also correlate well with IEPOX-SOA$_{PMF}$ in SOAS-CTR and could be potential tracers for IEPOX-SOA$_{PMF}$. However, scatter plots between these four ions and $C_5H_6O^+$ at different campaigns indicate they either have higher background values or lower signal-to-noise compared to $C_5H_6O^+$ (Fig. S5).

$f_{C_5H_6O}^{IEPOX\text{-}SOA}$ from SOAS and other field and laboratory studies (Table 1) ranges from 12 to 40 ‰ (‰ = parts per thousand) and have an average value of $22 \pm 7$ ‰. The average $f_{C_5H_6O}^{IEPOX\text{-}SOA}$ value shown here also includes $f_{82}$ data from four UMR IEPOX-SOA$_{PMF}$ spectra. This is justified since $C_5H_6O^+$ accounts for over 95 % of $m/z$ 82 in IEPOX-SOA based on results from SOAS-CTR and other lab studies (Kuwata et al., 2015). Indeed the average does not change if the UMR studies are removed from the average. These values are substantially higher than those from other types of OA or from locations with little impact from IEPOX-SOA, as discussed below.

### 3.2 $f_{C_5H_6O}$ in areas with strong influence from urban and biomass-burning emissions

We next examine whether primary organic aerosol (POA) or SOA from field studies in areas strongly influenced by urban and biomass-burning emissions and without substantial predicted gas-phase IEPOX concentrations or IEPOX-SOA contributions can lead to enhanced $f_{C_5H_6O}^{OA}$. Figure 3a shows the distribution of $f_{C_5H_6O}^{OA}$ in this category of studies peaks at $1.7 \pm 0.1$ ‰ (range 0.02–3.5 ‰). Data from continental air masses sampled from aircraft over the western and northwest USA (where isoprene emissions are low) are shown in Fig. 3b and show a similar range as the polluted ground sites.

Biomass-burning emissions and plumes sampled over multiple studies show a similar range to the pollution studies, with some slightly higher values. The peak of the distribution of $f_{C_5H_6O}^{OA}$ from fresh biomass-burning smoke across many different biomasses during the FLAME-3 study is 2.0 ‰. During the SEAC4RS aircraft campaign, many biomass-burning plumes were sampled, where OA concentrations varied over a wide range (several tens to more than one thousand $\mu g\,m^{-3}$). The average $f_{C_5H_6O}^{OA}$ across these biomass-burning plumes was 1.75 ‰ with low variability ($\sim$ 20 %), see Fig. S6.

We also explore whether other anthropogenic POA emission sources could elevate $f_{C_5H_6O}$ above the observed background levels of $\sim$ 1.7 ‰. Figure 3c shows $f_{C_5H_6O}$ for POA spectra from vehicle exhaust, cooking, coal combustion, and multiple pure chemical standards (e.g., some alcohols; di- or poly acids) (Canagaratna et al., 2015). Almost all the values are below 2 ‰, with exceptions for one type of cooking POA at 3 ‰, the polyol xylitol (4.2 ‰), and some acids (5-Oxoazelaic acid = 4.8 ‰, Gamma ketopimelic acid = 5.2 ‰, ketopimelic acid = 6.5 ‰, 3-Hydroxy-3-Methylglutaric acid = 11.8 ‰, Adipic acid = 16.4 ‰). All the tracers resulting in elevated $f_{C_5H_6O}$ contain multiple hydroxyl groups, and may result in furan-like structures

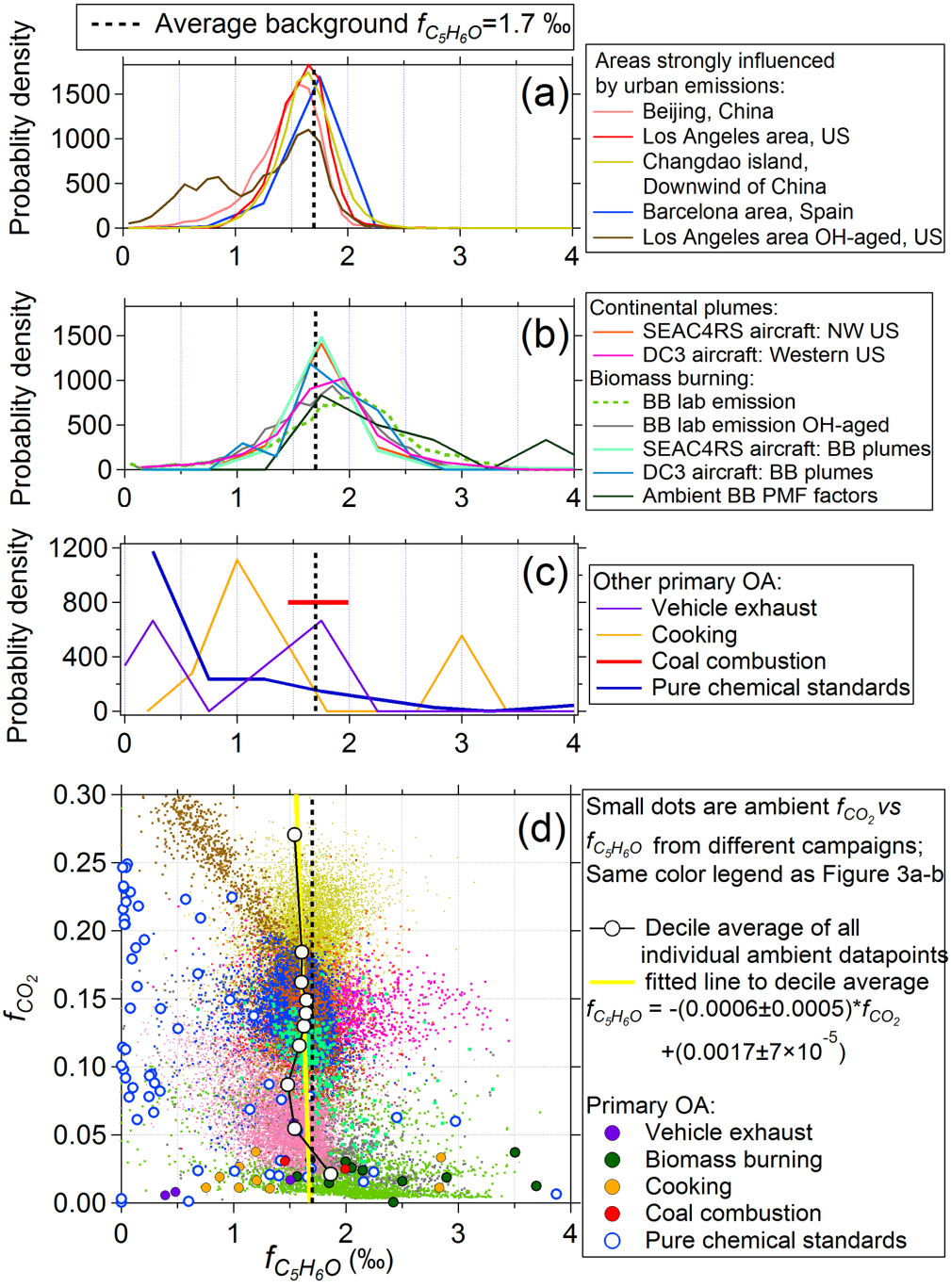


**Figure 3.** Probability density distributions of $f_{C_5H_6O}$ in studies **(a)** strongly influenced by urban emissions; **(b)** continental air masses sampled from aircraft and biomass-burning emissions; **(c)** other anthropogenic primary OA sources and pure chemical standards. The dashed line (1.7 ‰) is the average $f_{C_5H_6O}$ in studies shown in panels **(a)**–**(b)**. **(d)** Scatter plot of $f_{CO_2}$ ($f_{CO_2} = CO_2^+/OA$) vs. $f_{C_5H_6O}$ for all studies shown in panels **(a)**–**(c)**, using the same color scheme. Quantile averages of $f_{C_5H_6O}$ across all studies sorted by $f_{CO_2}$ are also shown, as is a linear regression line to the quantile points.

via facile dehydration reactions (Canagaratna et al., 2015). Xylitol has been proposed as a tracer of toluene SOA (Hu et al., 2008). It has a similar structure to 2-methyltetrols, with 5-OH groups instead of 4. In the AMS, xylitol may form the methylfuran structure through dehydration reactions like 2-methytetrols. However, $f_{C_5H_6O}$ in other toluene SOA tracers in our data set show background levels of $f_{C_5H_6O}$ ($< 2$ ‰). Given the small fraction of xylitol in toluene SOA (Hu et al., 2008), xylitol is unlikely to increase $f_{C_5H_6O}$ in anthropogenic SOA, consistent with our results.

In summary, in the absence of strong impacts from biogenic SOA, the AMS high-resolution ion $C_5H_6O^+$ has a clear and stable background, spanning a small range (0.02–3.5 ‰) with an average value around $1.7 \pm 0.1$ ‰ ($f^{\text{OA-Bkg-UB}}_{C_5H_6O}$), about an order of magnitude lower than the average value ($22 \pm 7$ ‰) of $f^{\text{IEPOX-SOA}}_{C_5H_6O}$.

### 3.3 Enhancements of $f_{C_5H_6O}$ in areas strongly influenced by isoprene emissions

GEOS-Chem predicts much higher surface gas-phase IEPOX concentrations over the SE USA and Amazon rainforest than those in temperate urban areas (Fig. 1). This is expected from high isoprene concentrations (e.g. 3.3 ppb in SOAS-CTR and 4 ppb in the Amazon) under low average NO concentrations ($\sim 0.1$ ppb) (Karl et al., 2009; Ebben et al., 2011). Probability distributions of $f^{\text{OA}}_{C_5H_6O}$ during both campaigns are shown in Fig. 4a, and are very similar with averages of 5–6 ‰ (range 2.5–11 ‰). The Amazon forest downwind of Manaus and a Borneo tropical forest study show even higher averages of 7 and 10 ‰, respectively (Robinson et al., 2011; de Sá et al., 2015). During the SEAC4RS aircraft campaign, the average $f^{\text{OA}}_{C_5H_6O}$ ($4.4 \pm 1.6$ ‰) from all SE US flights is also enhanced compared to levels observed in the northwest and western USA continental air masses ($1.7 \pm 0.3$ ‰) where isoprene emissions are much smaller (Guenther et al., 2012). Thus, campaigns in locations strongly influenced by isoprene emissions under lower NO conditions show systematically higher $f^{\text{OA}}_{C_5H_6O}$ values (with an average peak of $6.5 \pm 2.2$ ‰) than background levels found in other locations (1.7 ‰). The fact that $f^{\text{OA}}_{C_5H_6O}$ ($6.5 \pm 2.2$ ‰) in these studies is lower than the values in IEPOX-SOA ($22 \pm 7$ ‰) is expected, since ambient data sets also include OA from other sources, and confirms that IEPOX-SOA is not an overwhelmingly dominant OA source at most of those locations (see Fig. S7).

### 3.4 Values of $f_{C_5H_6O}$ in laboratory studies of non-IEPOX-derived isoprene SOA

We also investigate $f_{C_5H_6O}$ in laboratory SOA from isoprene in Fig. 4a. For SOA produced by chamber isoprene photooxidation under high-$NO_x$ conditions, low $f_{C_5H_6O}$ ($< 2$ ‰) within the background level is observed (Kroll et al., 2006; Chen et al., 2011). SOA from oxidation of isoprene hydroxyhydroperoxide (ISOPOOH; a product of low-NO oxidation of isoprene) under low-NO conditions, when formed under conditions that are not favorable for the reactive uptake of IEPOX into aerosols also has low $f_{C_5H_6O}$ of 2 ‰ (Krechmer et al., 2015). Low values of $f_{C_5H_6O}$ ($< 3$ ‰) are also observed in SOA from isoprene + $NO_3$ radical reactions without acid seeds (Ng et al., 2008). The low $f_{C_5H_6O}$ ($< 3$ ‰) observed in non-IEPOX-derived isoprene SOA indicate that $f_{C_5H_6O}$ is specifically enhanced from IEPOX-SOA, and is not a tracer for all SOA from isoprene.

### 3.5 Enhancements of $f_{C_5H_6O}$ in areas strongly influenced by monoterpene emissions

The BEACHON-RoMBAS campaign was carried out in a Rocky Mountain pine forest with high monoterpene emissions that account for 34 % in daytime and 66 % at night of the total volatile organic compound (VOC) mixing ratios (on average peaking at 0.15 ppb during day and 0.7 ppb at night) (Fry et al., 2013) but lower isoprene emissions (peaking at 0.35 ppb during daytime) (Kaser et al., 2013; Karl et al., 2014). One-third of the $RO_2$ radicals react via the low-NO route (i.e. via $RO_2 + HO_2$) at this site (Fry et al., 2013). The isoprene / monoterpene ratio at the Rocky Mountain site is 0.48, and is $\sim$ 10–20 times lower than the value (4.7) in SOAS-CTR and (8.3) in Amazon studies (Chen et al., 2015), suggesting that $f^{\text{OA}}_{C_5H_6O}$ may be near background levels because of the very low potential contribution of IEPOX-SOA at the Rocky Mountain site. However, the average $f^{\text{OA}}_{C_5H_6O}$ at the Rocky Mountain site is $3.7 \pm 0.5$ ‰ (Fig. 4a), which although lower than the average $f^{\text{OA}}_{C_5H_6O}$ (6.5 ‰) found in the SE US-CTR, Amazon, and Borneo forests, it is still twice the $f^{\text{OA-Bkg-UB}}_{C_5H_6O}$ value of 1.7 ‰ observed in pollution and smoke-dominated locations.

Three circumstances may lead to such an enhanced $f^{\text{OA}}_{C_5H_6O}$ at the Rocky Mountain site, which we examine here.

1. A small amount of IEPOX-SOA may be formed from the limited isoprene present at the Rocky Mountain site and surrounding region. However, the average isoprene concentration in this pine forest area is only 0.2 ppb, which is around 16 times less than that (3.3 ppb) at the SE US site in SOAS. The conditions at the Rocky Mountain site were less favorable for IEPOX-SOA formation due to a higher fraction (70 % in daytime) of the $RO_2$ radicals reacting with NO and less acidic aerosols (Fry et al., 2013; Levin et al., 2014). Thus, we can estimate an upper limit contribution of IEPOX-SOA to the $f^{\text{OA}}_{C_5H_6O}$ tracer at the Rocky Mountain site assuming the same ratio of IEPOX-SOA to isoprene in both campaigns. In this case, we would expect $f^{\text{OA}}_{C_5H_6O}$ at the Rocky Mountain site to be the background level (1.7 ‰) plus 1/16th of the enhancement above the background observed in SOAS ($5‰ - 1.7 = 3.3$ ‰) multiplied by the ratio of OA concentrations at both sites ($4.8\,\mu g\,m^{-3}$ in SE US site vs. $1.8\,\mu g\,m^{-3}$ in Rocky Mountain site). This calculation results in an expected

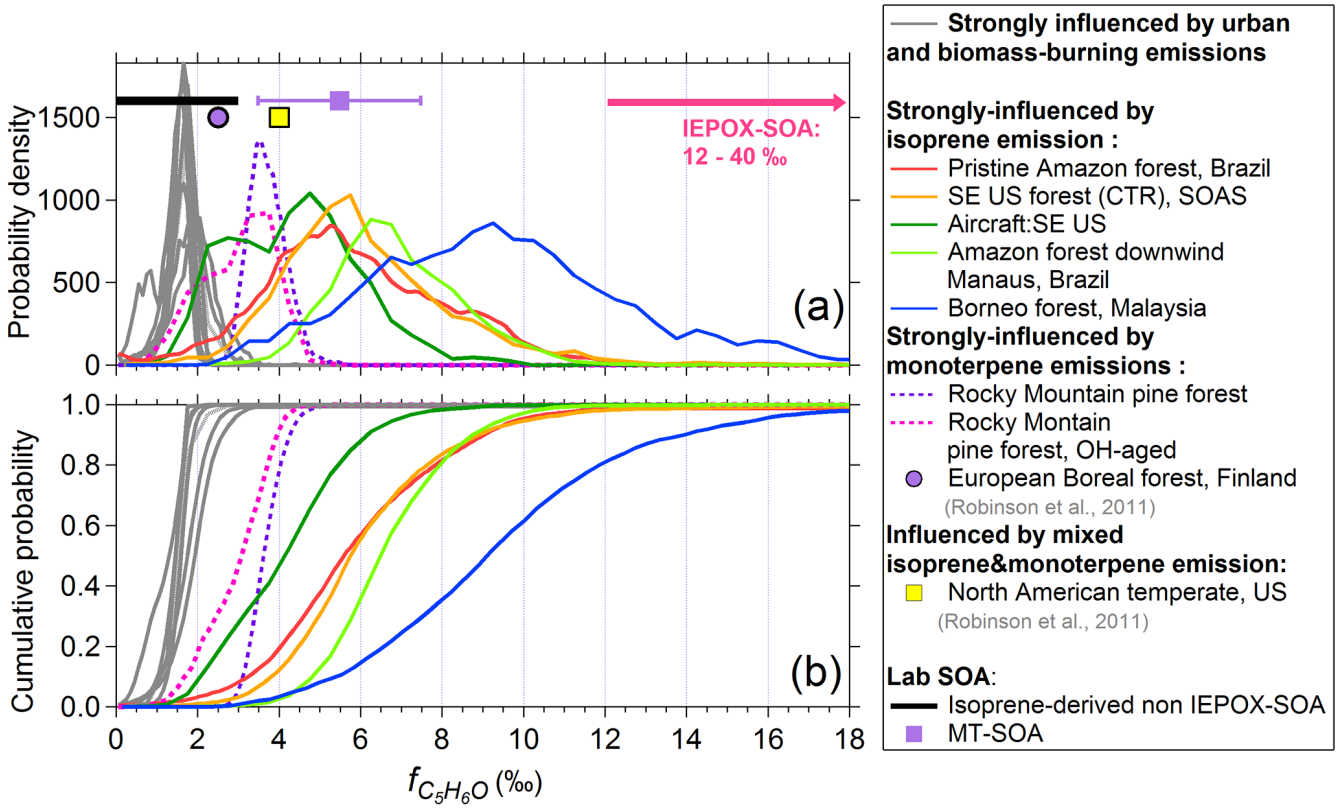


**Figure 4. (a)** Probability density and **(b)** cumulative probability distributions of $f^{OA}_{C_5H_6O}$ in studies strongly influenced by isoprene and/or monoterpene emissions. The ranges of $f_{C_5H_6O}$ from other non-IEPOX-derived isoprene-SOA and MT-SOA are also shown. The background grey lines are from studies strongly influenced by urban and biomass-burning emissions and are the same data from Fig. 3a–b. The arrow in Fig. 4a indicates the range of $f^{IEPOX\text{-}SOA}_{C_5H_6O}$ between 12 ‰ (start of the arrow) to 40 ‰ which is beyond the range of $x$ axis scale.

upper limit $f^{OA}_{C_5H_6O} \sim 2.25$ ‰ at the Rocky Mountain site due to the IEPOX-SOA contribution. This estimate is much lower than the observed average 3.7 ‰. Thus, the elevated $f^{OA}_{C_5H_6O}$ in Rocky Mountain pine forest is very unlikely to be due to IEPOX-SOA.

2. The second explanation of high $f^{OA}_{C_5H_6O}$ observed at Rocky Mountain site is that SOA from monoterpene oxidation (MT-SOA) may have a higher $f_{C_5H_6O}$ than background OA from other sources. MT-SOA is thought to compose a major fraction of the OA at the site. Several chamber studies show that MT-SOA, e.g., SOA from ozonolysis (Chhabra et al., 2011; Chen et al., 2015) or photo-oxidation (Ng et al., 2007) of $\alpha$-pinene, or $NO_3$ reaction with $\alpha$-pinene, or $NO_3$ reaction with $\alpha$-pinene, $\beta$-pinene, and $\Delta^3$-Carene (Fry et al., 2014; Boyd et al., 2015) can result in higher $f_{C_5H_6O}$ (average $5.5 \pm 2.0$ ‰) than background levels of $\sim 1.7$ ‰ (Fig. 4a). We note that the average lab-generated MT-SOA value ($f^{MT\text{-}SOA}_{C_5H_6O}$) is still 4 times lower than the average $f^{IEPOX\text{-}SOA}_{C_5H_6O}$ for IEPOX-SOA$_{PMF}$ and IEPOX-SOA$_{lab}$ (Fig. S8), and thus there is some room to separate both contributions. Oxidation of monoterpenes can lead to species with multiple –OH groups, which may result in the production of methylfuran (or ions of similar structure) upon AMS analysis. We do not observe enhanced $f_{C_5H_6O}$ in SOA from sesquiterpene oxidation ($< 2$ ‰) (Chen et al., 2015). The values of $f^{MT\text{-}SOA}_{C_5H_6O}$ in chamber studies, together with the finding of a substantial contribution of monoterpenes to SOA at this Rocky Mountain site (Fry et al., 2013) suggest that MT-SOA may explain the values of $f^{OA}_{C_5H_6O}$ observed there.

Two other field studies support the conclusion that ambient MT-SOA may have slightly enhanced $f_{C_5H_6O}$. Figure 6 shows data from a DC3 aircraft flight in the areas around Missouri and Illinois. Ambient $f^{OA}_{C_5H_6O}$ increases from background levels ($\sim 1.7$ ‰) to $\sim 4.1$ ‰ in a highly correlated manner to monoterpene concentration increases (with an average of 3.0 ‰ during the enhanced period). Meanwhile, isoprene and gas-phase IEPOX stay at low levels similar to the rest of the flight, indicating that enhanced $f^{OA}_{C_5H_6O}$ in the periods with higher MT concentrations should arise from MT-SOA and not IEPOX-SOA. Figure 4a includes AMS measurements at a MT emission-dominated Euro-

pean boreal forest (Hyytiälä, Finland) (Robinson et al., 2011). Average $f^{OA}_{C_5H_6O}$ is ~2.5 ‰ at this site, which is again higher than the $f^{OA\text{-}Bkg\text{-}UB}_{C_5H_6O}$ value of 1.7 ‰. The slightly lower $f^{OA}_{C_5H_6O}$ in the Boreal forest vs. the Rocky Mountain site may be partially explained by a small contribution from IEPOX-SOA at the latter (estimated above to increase $f^{OA}_{C_5H_6O}$ up to 2.25 ‰ at the Rocky Mountain site), as well as by differences of the MT-SOA / OA ratio at both sites (Corrigan et al., 2013) and the relative importance of different MT species and oxidation pathways.

3. The enhanced $f^{OA}_{C_5H_6O}$ at the Rocky Mountain site may have arisen from oxidation products of 2-methyl-3-buten-2-ol (MBO; $C_5H_{10}O$) emitted from pine trees. MBO, with a daytime average of 2 ppb accounts for ~50 % of the total VOC mixing ratio during the day (Karl et al., 2014). MBO has been shown to form aerosol with a 2–7 % yield in chamber studies, which is thought to proceed via the uptake of epoxide intermediates ($C_5H_{10}O_2$, vs. IEPOX $C_5H_{10}O_3$) under acidic aerosol conditions (Zhang et al., 2012, 2014; Mael et al., 2014). Some aerosol species formed by MBO-derived epoxides have similar structures (e.g., $C_5H_{12}O_3$) to the IEPOX oxidation products in SOA and thus they might contribute to $f^{OA}_{C_5H_6O}$. No pure MBO-derived epoxides or their oxidation products in the aerosol phase have been measured by AMS so far, to our knowledge.

   To attempt to differentiate whether MT-SOA or MBO-SOA dominate the higher $f^{OA}_{C_5H_6O}$ at the Rocky Mountain site, average diurnal variations of ambient $f^{OA}_{C_5H_6O}$, monoterpene, and isoprene + MBO are plotted in Fig. S9. $f^{OA}_{C_5H_6O}$ shows a diurnal pattern that increases at night and peaks in the early morning, similar to the diurnal variation of monoterpenes. Monoterpenes continue to be oxidized during nighttime at this site by $NO_3$ radical and $O_3$ with a lifetime of ~30 min (with 5 ppt of $NO_3$ and 30 ppb of $O_3$) (Fry et al., 2013). In contrast only a decrease and later a plateau of $f^{OA}_{C_5H_6O}$ are observed during the period with high MBO concentration and higher oxidation rate of MBO due to high OH radical in daytime (as MBO reacts slowly with $O_3$ and $NO_3$) (Atkinson and Arey, 2003). While MBO-SOA may or may not have $f_{C_5H_6O}$ above background levels, the diurnal variations point to MT-SOA playing a dominant role in $f^{OA}_{C_5H_6O}$ at this site.

   The average $f^{OA}_{C_5H_6O}$ in areas strongly influenced by monoterpene emissions is $3.1 \pm 0.6$ ‰, obtained by averaging the values from the Rocky mountain forest (3.7 ‰), European boreal forest (2.5 ‰), and DC3 flight (3.0 ‰). Note that the difference between $f^{OA}_{C_5H_6O}$ in areas strongly influenced by monoterpene emissions ($3.1 \pm 0.6$ ‰) and isoprene emissions ($6.5 \pm 2.2$ ‰) is reduced, compared to a factor of 4 differences between pure MT-SOA ($5.5 \pm 2.0$ ‰) and IEPOX-SOA ($22 \pm 7$ ‰). This is likely due to the physical mixing of OA from different sources and in different proportions at each location.

### 3.6 $f_{C_5H_6O}$ vs. OA oxidation level ($f_{CO_2}$) *triangle plot* – background studies

In AMS spectra, the $CO_2^+$ ion is a marker of aging and oxidation processes (Alfarra et al., 2004; Ng et al., 2011a). To evaluate whether oxidation plays a role on the observed $f_{C_5H_6O}$ for different types of OA, in this section we use plots of $f_{CO_2}$ (i.e., $CO_2^+$/OA) vs. $f_{C_5H_6O}$ as a graphical diagnostic of this process, similar to graphical diagnostics (triangle plots) used for other purposes with AMS data (Cubison et al., 2011; Ng et al., 2011a). For studies strongly influenced by urban and biomass-burning emissions in Fig. 3d, we observe a wide range of $f^{OA}_{CO_2}$ values from 0.001 to 0.3 (i.e., 30 % or 300 ‰). The wide range of $f^{OA}_{CO_2}$ is due to variable fractions of POA and SOA (mixing effect) and a variable oxidation level of POA and SOA (oxidation effect) in the different studies. In fact, to our knowledge, these studies encompass the values of $f^{OA}_{CO_2}$ observed in all ambient AMS studies to date (Ng et al., 2011a). Several studies where urban and forest air or biomass-burning smoke were aged by intense OH oxidation with an oxidation flow reactor (OFR) (Kang et al., 2007; Li et al., 2013; Ortega et al., 2013) are also included. However, despite the wide range of $f^{OA}_{CO_2}$, $f^{OA}_{C_5H_6O}$ changes little, staying in the range 0.02–3.5 ‰, and with little apparent dependence on $f^{OA}_{CO_2}$ for the ambient studies. A linear regression to quantiles from this data set results in an intercept of 1.7 ‰ and a very weak decrease with increasing $f^{OA}_{CO_2}$. A stronger decrease is observed when aging urban air (Los Angeles) by intense OH exposure in flow reactor, as shown in Fig. 3d.

Ambient $f^{OA}_{CO_2}$ at the Rocky Mountain forest site shows a moderate oxidation level (0.1–0.15), similar to the SE US-CTR (Fig. 5). $f^{OA}_{C_5H_6O}$ in the Rocky mountain site decreases linearly when $f^{OA}_{CO_2}$ increases. During the Rocky Mountain study, the intense OH aging of ambient air in a flow reactor shows a continuation of the trend observed for the ambient data, where $f^{OA}_{C_5H_6O}$ decreases as $f^{OA}_{CO_2}$ increases. A linear regression to the combined ambient and OFR data sets ($f^{OA}_{C_5H_6O} = -0.013 \times f^{OA}_{CO_2} + 0.0054$) will be used below to estimate background $f^{OA}_{C_5H_6O}$ in areas with strong monoterpene and low isoprene emissions.

$f_{C_5H_6O}$ in ambient SOA from other studies catalogued in the HR-AMS spectral database are also shown in Fig. 5. Most urban oxygenated OA (OOA) are within $f^{OA\text{-}Bkg\text{-}UB}_{C_5H_6O}$ (average 1.7 ‰; range: 0.02–3.5 ‰), which is consistent with the $f_{C_5H_6O}$ (< 3 ‰) in lab aromatic SOA and other urban OA in Fig. 5. However, some ambient SOA spectra do show higher $f_{C_5H_6O}$ (3–10 ‰) than the $f^{OA\text{-}Bkg\text{-}UB}_{C_5H_6O}$ (0.02–3.5 ‰), which we will discuss in the next section.

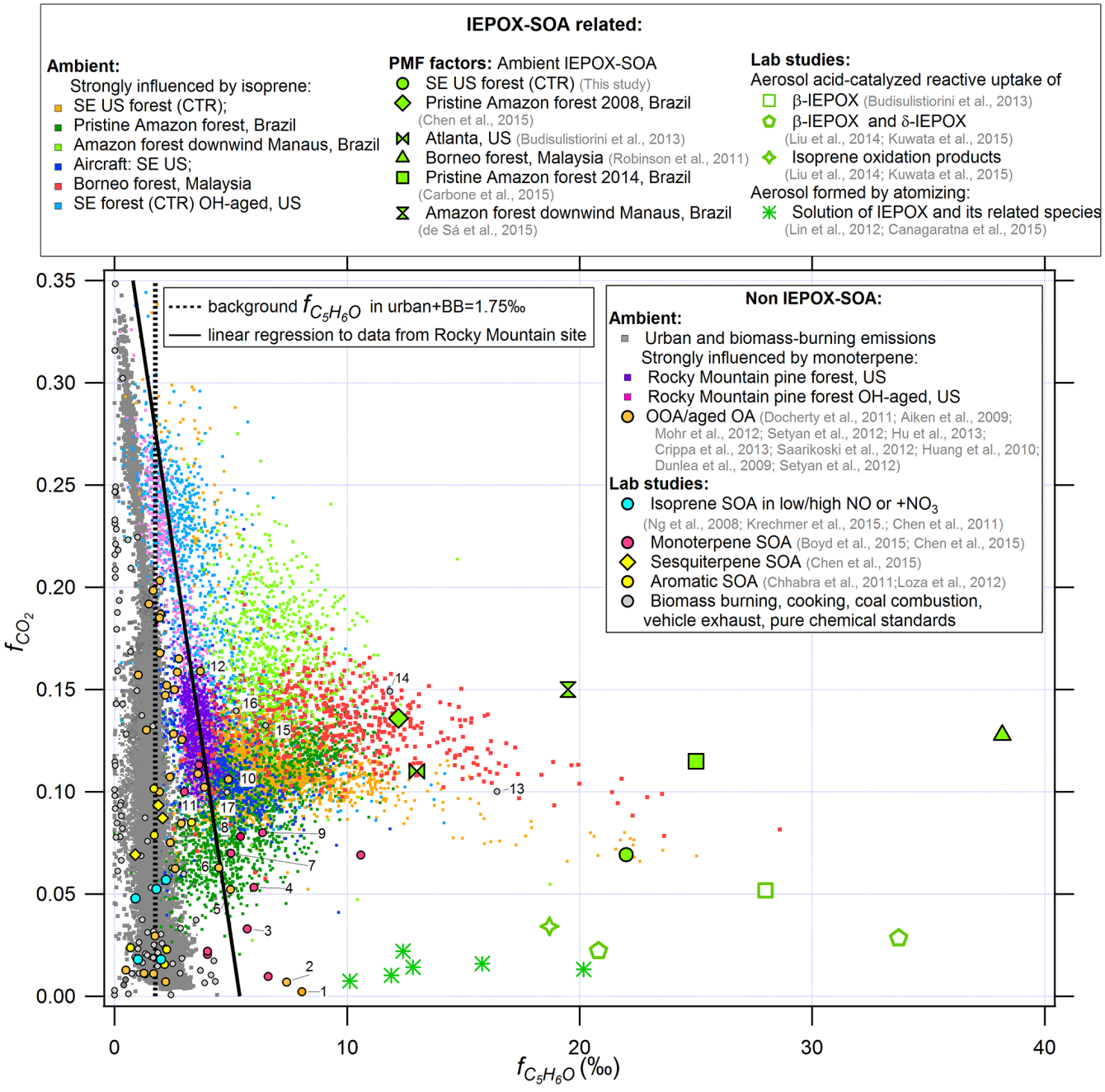


**Figure 5.** Scatter plot of $f_{CO_2}$ and $f_{C_5H_6O}$ in studies strongly by isoprene and monoterpene emissions, as well as other OA sources. The grey dots represent background levels from studies strongly influenced by urban and biomass-burning emissions in Fig. 3d. $f_{CO_2}$ and $f_{C_5H_6O}$ values from multiple sources of OA are also shown, together with IEPOX-SOA from different ambient PMF factors and chamber studies. A linear regression line of $f_{CO_2}$ and $f_{C_5H_6O}$ calculated from Rocky Mountain pine forest is also displayed. We labeled some symbols with high $f_{C_5H_6O}$ in numbers. Numbers 1–12 are all OAs with biogenic influences. Numbers 13–17 are some pure chemical standards (acids) as discussed above. For detailed information on the meaning of the numbered symbols see supporting information Table S2.

### 3.7 $f_{C_5H_6O}$ vs. OA oxidation level ($f_{CO_2}$) – IEPOX-SOA-influenced studies

$f^{OA}_{CO_2}$ vs. $f^{OA}_{C_5H_6O}$ in studies impacted by IEPOX-SOA are shown in Fig. 5. Consistent with the distributions discussed above, the bulk of points from these areas all show distinctively enhanced $f^{OA}_{C_5H_6O}$ when compared to background $f^{OA}_{C_5H_6O}$ points of similarly moderate or higher oxidation levels. The $f^{OA}_{C_5H_6O}$ measurements with lower $f^{OA}_{CO_2}$ values are

more broadly distributed than the $f^{OA}_{C_5H_6O}$ points with higher $f^{OA}_{CO_2}$ values in SE US-CTR, SEAC4RS, Borneo forest, and Amazon forest downwind of Manaus. However, increased $f^{OA}_{C_5H_6O}$ with higher $f^{OA}_{CO_2}$ was observed in the Amazon. Both oxidation and mixing of air masses with different OA can influence these observations. $f^{IEPOX\text{-}SOA}_{C_5H_6O}$ in IEPOX-SOA usually will decrease with oxidative aging. For example, $f^{OA}_{C_5H_6O}$ from the SOAS oxidation flow reactor decreases continuously as OA becomes more oxidized than ambient OA in SOAS-CTR ($f^{OA}_{CO_2}$ increases from 0.15 to 0.3). Air mass mixing effects are more complex. Depending on the $f^{OA}_{CO_2}$ in the air masses it is mixed with, $f^{OA}_{C_5H_6O}$ in IEPOX-SOA-rich air can show positive, neutral or negative trends with increasing $f^{OA}_{CO_2}$. For example, in pristine Amazon forest, points with both lower $f^{OA}_{CO_2}$ ($< 0.08$) and $f^{OA}_{C_5H_6O}$ ($< 8$ ‰) values are thought to be mainly caused by advection of POA from occasional local pollution.

The overall trend for the ambient measurements in studies strongly influenced by isoprene emissions (Fig. 5) is that those points cluster in a triangle shape and $f^{OA}_{C_5H_6O}$ decreases as $f^{OA}_{CO_2}$ increases, as illustrated in Fig. S10. This "triangle shape" indicates that as the ambient OA oxidation increases, the IEPOX-SOA signature is reduced, potentially by the ambient oxidation processes or by physical mixing with air masses containing more aged aerosols.

Finally, points with higher $f_{C_5H_6O}$ in OOA/aged OA are labeled with numbers in Fig. 5. The sources of those labeled points are summarized in Table S2 in the Supplement. OA from those studies are all partially influenced by biogenic emissions. For example, during measurements of ambient OA in the Central Valley of California (number 2), high isoprene emissions and acidic particles were observed (Dunlea et al., 2009), suggesting that potential IEPOX-SOA formed in this area may explain the higher $f^{OA}_{C_5H_6O}$ there.

### 3.8 Best estimate of $f_{C_5H_6O}$ in IEPOX-SOA

IEPOX-SOA from different field campaigns and chamber studies lay towards the right and on the bottom half of Fig. 5. IEPOX-SOA from chamber studies show systematically lower $f^{IEPOX\text{-}SOA}_{CO_2}$ than ambient studies. This is likely explained by the lack of additional aging in the laboratory studies, because all the lab IEPOX-SOA were measured directly after uptake gas-phase IEPOX onto acidic aerosol without undergoing substantial additional oxidation.

A wide range (12–40 ‰) of $f^{IEPOX\text{-}SOA}_{C_5H_6O}$ is observed with an average of 22 ‰ ± 7 ‰ in ambient and lab IEPOX-SOA. $f^{IEPOX\text{-}SOA}_{C_5H_6O}$ did not show a trend vs. $f^{IEPOX\text{-}SOA}_{CO_2}$. The IEPOX-SOA molecular tracer 3-MeTHF-3,4-diols has been shown to enhance the $f_{C_5H_6O}$ in OA (Fig. 5) (Lin et al., 2012; Canagaratna et al., 2015). Except for 3-MeTHF-3,4-diols none of the other pure IEPOX-derived polyols standards have been atomized and injected into the AMS system so far, to our knowledge. We suspect other polyols such as 2-methyltetrols may also lead to such an enhancement through dehydration reactions in the AMS vaporizer leading to methylfuran-type structures. The diversity of $f^{IEPOX\text{-}SOA}_{C_5H_6O}$ in different studies is related to the variable content of specific IEPOX-SOA molecular species that enhance $f^{IEPOX\text{-}SOA}_{C_5H_6O}$ differently. The fractions of molecular IEPOX-SOA species in total IEPOX-SOA$_{PMF}$ is plotted vs. $f^{IEPOX\text{-}SOA}_{C_5H_6O}$ in three different studies in Fig. 7, which show a strong correlation between each other. The strong simultaneous variation of both quantities indicates that the diversity of $f^{IEPOX\text{-}SOA}_{C_5H_6O}$ is very likely explained by the variability of the molecules comprising IEPOX-SOA among different studies.

During 1 day in SOAS (26 June 2013), IEPOX-SOA$_{PMF}$ comprised 80–90 % of total OA (Fig. S11), possibly due to high sulfate concentrations favoring IEPOX-SOA formation. $f^{OA}_{C_5H_6O}$ reached 25 ‰, which is similar to the 22 ‰ for the IEPOX-SOA$_{PMF}$ from this study, and consistent with a slightly lower value for the average vs. freshest ambient IEPOX-SOA. Among the chamber studies, the study of reactive uptake of isoprene oxidation products into an acidic seed is most similar to the full chemistry in real ambient environments (Liu et al., 2014), and reports similar $f^{IEPOX\text{-}SOA}_{C_5H_6O}$ values (19 ‰). Hence, we propose an average $f^{IEPOX\text{-}SOA}_{C_5H_6O}$ (22 ‰) from both studies as the typical value of fresh IEPOX-SOA.

### 3.9 Proposed method for real-time estimation of IEPOX-SOA

So far, PMF of AMS spectra is the only demonstrated method for quantifying total IEPOX-SOA concentrations. However, the PMF method is labor intensive and requires significant expertise, and may fail to resolve a certain factor when present in lower mass fractions ($< 5$ %). A simpler, real-time method to estimate IEPOX-SOA would be useful in many studies, including ground-based and aircraft campaigns.

We propose an estimation method for IEPOX-SOA based on the mass concentration of its tracer ion $C_5H_6O^+$. To do this, we express the mass concentration of $C_5H_6O^+$ as

$$C_5H_6O^+_{total} = C_5H_6O^+_{IEPOX\text{-}SOA,ambient} + C_5H_6O^+_{background}, \quad (1)$$

where $C_5H_6O^+_{total}$ is measured total $C_5H_6O^+$ signal in AMS, $C_5H_6O_{IEPOX\text{-}SOA,ambient}$ and $C_5H_6O^+_{background}$ are the $C_5H_6O^+$ signals contributed by IEPOX-SOA in ambient OA and other background OA (non-IEPOX-SOA).

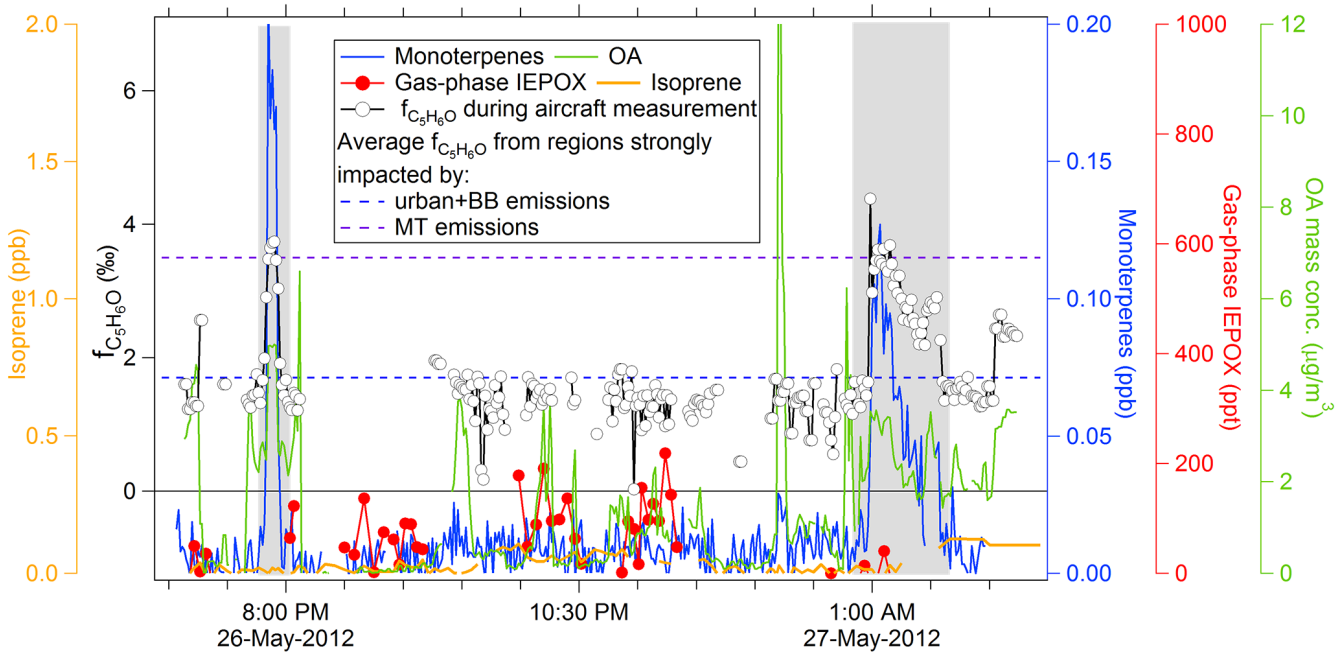


**Figure 6.** Time series of ambient $f^{OA}_{C_5H_6O}$, gas-phase IEPOX, monoterpenes, and isoprene in DC3 aircraft measurement. Average $f_{C_5H_6O}$ from regions strongly impacted by urban and biomass-burning emissions and MT emissions are also shown for reference. Two areas with grey background indicate the periods when $f^{OA}_{C_5H_6O}$ increases when monoterpene concentrations increase.

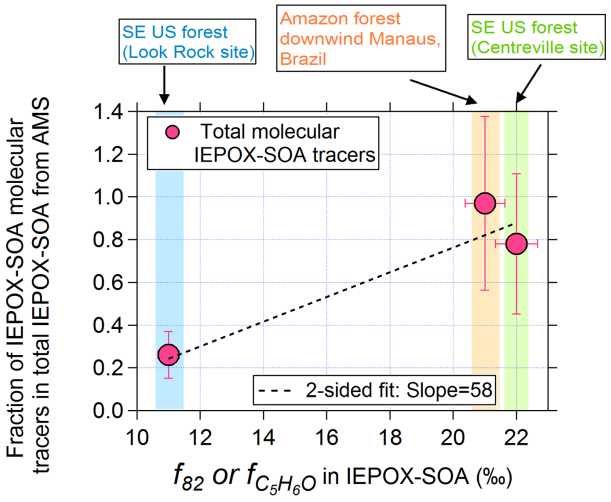


**Figure 7.** Scatter plot between total IEPOX-SOA molecular tracers (i.e., Methyltetrol + C5-alkene triols + IEPOX-derived organosulfates and dimers) in IEPOX-SOA$_{PMF}$ and $f^{IEPOX\text{-}SOA}_{82}$. Besides SOAS, the other two data sets in the graph are from Budisulistiorini et al. (2015) and de Sá et al. (2015). The relative uncertainty value estimated for the SOAS study is applied to the other two data sets.

Then, $C_5H_6O_{IEPOX\text{-}SOA,ambient}$ and $C_5H_6O^+_{background}$ can be calculated as

$$C_5H_6O^+_{IEPOX\text{-}SOA,ambient} = IEPOX\text{-}SOA \times f^{IEPOX\text{-}OA}_{C_5H_6O} \quad (2)$$

$$C_5H_6O^+_{background} = (OA_{mass} - IEPOX\text{-}SOA) \times f^{OA\text{-}Bkg}_{C_5H_6O}, \quad (3)$$

where $f^{IEPOX\text{-}OA}_{C_5H_6O}$ is the fractional contribution of $C_5H_6O^+$ to the total ion signal in the spectra of IEPOX-SOA from IEPOX-SOA$_{lab}$ or IEPOX-SOA$_{PMF}$ factors. $f^{OA\text{-}Bkg}_{C_5H_6O}$ is the background $f_{C_5H_6O}$ in other non-IEPOX-SOA, e.g., values from OA strongly influenced by urban and biomass-burning emissions ($f^{OA\text{-}Bkg\text{-}UB}_{C_5H_6O}$).

Then, by combining Eqs. (1)–(3), we can express $C_5H_6O^+_{total}$ as

$$C_5H_6O^+_{total} = IEPOX\text{-}SOA \times f^{IEPOX\text{-}OA}_{C_5H_6O} + (OA\text{-}IEPOX\text{-}SOA) \times f^{OA\text{-}Bkg}_{C_5H_6O}. \quad (4)$$

Finally, IEPOX-SOA can be estimated as

$$IEPOX\text{-}SOA = \frac{C_5H_6O^+_{total} - OA \times f^{OA\text{-}Bkg}_{C_5H_6O}}{f^{IEPOX\text{-}OA}_{C_5H_6O} - f^{OA\text{-}Bkg}_{C_5H_6O}}. \quad (5)$$

In Eq. (5), $C_5H_6O^+_{total}$ and OA mass are measured directly by AMS. $f^{OA\text{-}Bkg}_{C_5H_6O}$ and $f^{IEPOX\text{-}OA}_{C_5H_6O}$ are two parameters that must be determined by other means.

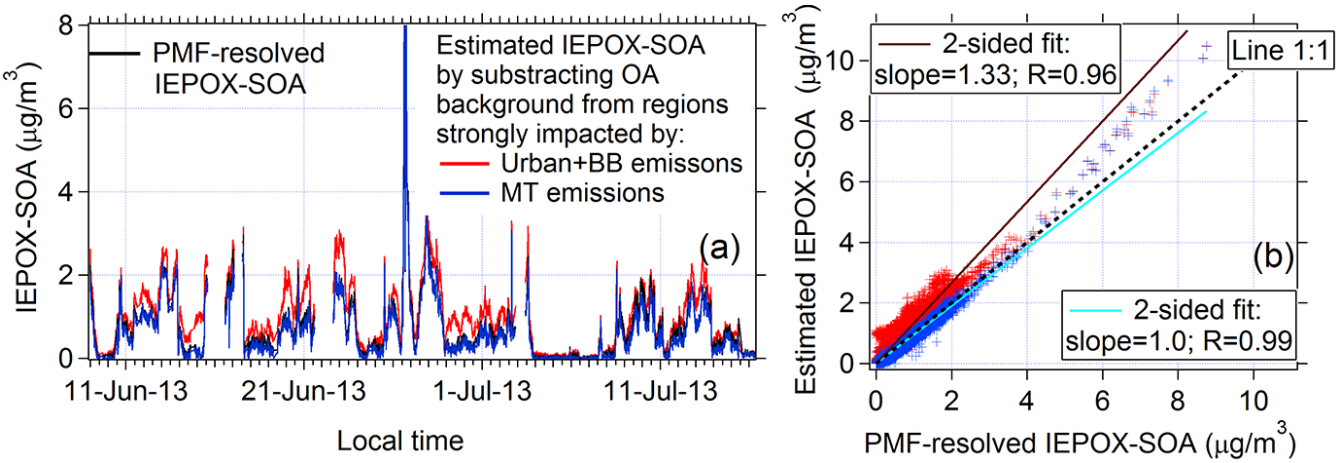


**Figure 8. (a)** Time series of IEPOX-SOA$_{PMF}$ and estimated IEPOX-SOA based on $C_5H_6O^+$ for the SOAS data in SE US. Two different estimates of background $C_5H_6O^+$ are shown, using values from regions strongly impacted by urban and biomass-burning emissions vs. regions with strong monoterpene emissions. **(b)** Scatter plot of estimated IEPOX-SOA vs. IEPOX-SOA$_{PMF}$. Note that the largest IEPOX-SOA plume on 26 June 2013 had a slightly higher $f^{OA}_{C_5H_6O}$ of 24 ‰, resulting in a slight overestimation of IEPOX-SOA for those data points.

As discussed above, the background value in the absence of a substantial impact of MT-SOA is ∼ 1.7 ‰. In studies influenced by monoterpene emissions, the background value may be elevated by MT-SOA. $f^{OA}_{C_5H_6O}$ at the Rocky Mountain site estimated by $f^{OA}_{C_5H_6O} = (0.41 - f^{OA}_{CO_2}) \times 0.013$ (Fig. 5) can be used as $f^{OA\text{-}Bkg}_{C_5H_6O}$ for areas with strong MT-SOA contributions ($f^{OA\text{-}Bkg\text{-}MT}_{C_5H_6O}$). There is some uncertainty in this value, due to possible contributions of a small amount of IEPOX-SOA, MBO-SOA, and other OA sources at this site. An alternative estimate for $f^{OA\text{-}Bkg\text{-}MT}_{C_5H_6O}$ would be $\sim 1.7‰ + 3 \times MT_{avg}$ (ppb), which is also approximately consistent with our ambient data, but may have higher uncertainty. Further characterization of the background $f_{C_5H_6O}$ in areas with MT-SOA impact is of interest for future studies. Finally, we have decided to use $f^{OA}_{C_5H_6O}$ estimated from the Rocky Mountain site as $f^{OA\text{-}Bkg\text{-}MT}_{C_5H_6O}$ in the following calculation. As discussed above, we use average $f^{IEPOX\text{-}OA}_{C_5H_6O} = 22‰$ in Eq. (3) as a representative value of ambient IEPOX-SOA. Several scenarios based on different $f^{OA}_{C_5H_6O}$ values to use this tracer-based method are addressed in the Supplement. The justification from users on using this method is needed.

### 3.10 Application of the real-time estimation method of IEPOX-SOA

To test the proposed estimation method, we use SE US forest (SOAS) data as an example in Fig. 8, applying both background estimates (urban and biomass burning, and monoterpene emissions). Since there are high monoterpene concentrations (∼ 1 ppb during the night) in SOAS, we expect the MT-influenced background to be more accurate. The IEPOX-SOA estimated by subtracting the MT-SOA background (IEPOX-SOA$_{MT}$) is indeed better correlated with IEPOX-SOA$_{PMF}$ ($R = 0.99$) than that ($R = 0.96$) when the urban and biomass-burning background is applied (IEPOX-SOA$_{urb\&bb}$). The intercept of regression line between IEPOX-SOA$_{MT}$ and IEPOX-SOA$_{PMF}$ is zero, indicating the background of IEPOX-SOA contributed by MT-SOA is clearly deducted.

The regression slope between IEPOX-SOA$_{MT}$ and IEPOX-SOA$_{PMF}$ is 0.95, suggesting that $C_5H_6O^+$ in SE US CTR site (SOAS) may be slightly overcorrected by minimizing $C_5H_6O^+$ from monoterpene emissions. This underestimation may be associated with higher MT-SOA contribution to $C_5H_6O^+$ at the Rocky Mountain pine forest site than at the SE US forest site, or interference from IEPOX-SOA/MBO-SOA at the Rocky Mountain site. IEPOX-SOA$_{urb\&bb}$ is 1.26 times higher than IEPOX-SOA$_{PMF}$. Thus, as expected IEPOX-SOA$_{MT}$ and IEPOX-SOA$_{urb\&bb}$ provide lower and upper limits of estimated IEPOX-SOA.

Among all the data sets introduced in this study, the SOAS-CTR data set should be the best case scenario since $f^{IEPOX\text{-}OA}_{C_5H_6O} = 22‰$ is coincidently the same value in the spectrum of IEPOX-SOA$_{PMF}$ in SOAS-CTR and a large fraction (17 %) of IEPOX-SOA existed in SOAS-CTR as well. Given the spread of values of $f^{IEPOX\text{-}OA}_{C_5H_6O}$ (12–40 ‰) in different studies, if no additional local IEPOX-SOA spectrum is available for a given site, the estimation from this method should be within a factor of ∼ 2 of the actual concentration, as illustrated in Figs. S13–S14. Further information concerning the estimation method using unit mass resolution $m/z$ 82 (or $f_{82}$) can be found in the Appendix A.

## 4 Conclusions

To investigate if the ion $C_5H_6O^+$ (at $m/z$ 82) in AMS spectra is a good tracer for IEPOX-SOA, tens of field and lab studies are combined and compared, including the SOAS 2013 campaign in the SE US. The results show that $f^{OA}_{C_5H_6O}$ is clearly elevated when IEPOX-SOA is present, and thus has potential usefulness as a tracer of this aerosol type. The average $f^{IEPOX\text{-}OA}_{C_5H_6O}$ in chamber and ambient studies is $22 \pm 7$ ‰ (range 12–40 ‰). No dependence of $f^{IEPOX\text{-}OA}_{C_5H_6O}$ on oxidation level ($f^{IEPOX\text{-}SOA}_{CO_2}$) was found. Background $f_{C_5H_6O}$ in OA strongly influenced by urban or biomass-burning emissions or pure anthropogenic POAs averages $1.7 \pm 0.1$ ‰ (range 0.02–3.5 ‰).

In ambient OA that is strongly influenced by isoprene emissions under lower NO, we observe systematically higher $f^{OA}_{C_5H_6O}$ (with an average of $\sim 6.5 \pm 2.2$ ‰), consistent with the presence of IEPOX-SOA. Low tracer values ($f_{C_5H_6O} < 3$ ‰) are observed in non-IEPOX-derived isoprene-SOA from laboratory studies, indicating that the tracer ion is specifically enhanced from IEPOX-SOA, and is not a tracer for all SOA from isoprene.

Higher background values of $f^{OA}_{C_5H_6O}$ ($3.1 \pm 0.6$ ‰ in average) were found in area strongly impacted by monoterpene emissions. $f^{MT\text{-}SOA}_{CO_2}$ is $5.5 \pm 2.0$ ‰, which are substantially lower than for IEPOX-SOA ($22 \pm 7$ ‰), and thus they leave some room to separate both contributions. A $f^{OA\text{-}Bkg\text{-}MT}_{C_5H_6O}$ as a function of $f^{OA}_{CO_2}$ in monoterpene emissions is determined by linear regressing the $f^{OA}_{C_5H_6O}$ and $f^{OA}_{CO_2}$ at a Rocky Mountain pine forest site.

A simplified method to estimate IEPOX-SOA based on measured ambient $C_5H_6O^+$, $CO_2^+$, and OA in AMS is proposed. Good correlations ($R > 0.96$) between estimated IEPOX-SOA and IEPOX-SOA$_{PMF}$ are obtained for SOAS, confirming the potential usefulness of this estimation method. Given the observed variability in IEPOX-SOA composition, the method is expected to be within a factor of $\sim 2$ of the true concentration if no additional information about the local IEPOX-SOA is available for a given study. When only unit mass-resolution data are available as in ACSM data, all methods may perform less well because of increased interferences from other ions at $m/z$ 82.

## Appendix A

In addition to the preceding high-resolution $C_5H_6O^+$ data analysis, we also investigated unit mass resolution (UMR) $m/z$ 82 as a tracer of IEPOX-SOA. In addition to $C_5H_6O^+$ ($m/z$ 82.0419), the reduced ion $C_6H_{10}^+$ and oxygenated ion $C_4H_2O_2^+$ often contribute signal to UMR $m/z$ 82. The average background level of $f_{82}^{OA}$ (i.e., $m/z$ 82/OA) is from $4.3 \pm 0.9$ ‰ (0.01 to 10 ‰) in studies strongly influenced by urban, biomass-burning, and other anthropogenic POA, as shown in Fig. A1a–c. This value is higher than the high-resolution $f_{C_5H_6O}^{OA\text{-}Bkg\text{-}UB}$ (1.7 ‰) in the same studies. Background $f_{82}^{OA}$ increases when OA is fresher (lower $f_{44}$, $f_{44}^{OA} = m/z$ 44/OA) as shown in Fig. A1d, and can be estimated as $f_{82}^{OA} = 5.5 \times 10^{-3} - 8.2 \times 10^{-3} \times f_{44}^{OA}$ in areas strongly impacted by urban and biomass-burning emissions. The uncertainty of calculated $f_{82}$ can be as high as 30 % in the lower fresh OA plumes by considering the uncertainties from quantile average and linear regression. There are also some pure chemical species that exhibit high $f_{82}$ values, as shown in Fig. A1c. These species include docosanol, eicosanol, and oleic acid. However, none of these pure chemical species alone contributes substantially to ambient aerosol.

The probability density distributions of $f_{82}^{OA}$ in studies strongly influenced by isoprene emissions are shown in Fig. A2a. The peaks ($\sim 8.7 \pm 2.5$ ‰) are similar in SE US, pristine, polluted Amazon forest, Borneo forest to high-resolution $f_{C_5H_6O}^{OA}$ ($\sim 6.5 \pm 2.2$ ‰), indicating $C_5H_6O^+$ is the dominant ion at UMR $m/z$ 82 in these studies. Compared to the studies with strong urban and biomass-burning emissions, clear enhancements of $f_{82}^{OA}$ in studies strongly influenced by isoprene emissions are still observed, but with less contrast than for in high-resolution data sets (Figs. A2–A3).

Figure A2a also shows the probability density distributions of $f_{82}^{OA}$ at Rocky Mountain and European boreal forests (strongly influenced by monoterpene emissions). Those distributions peak at $\sim 5$ ‰, which are within the range (0.01–10 ‰) of $f_{82}^{OA}$ in aerosols strongly influenced by urban and biomass-burning emissions. In the lab studies, most of $f_{82}^{MT\text{-}SOA}$ (average $6.7 \pm 2.2$ ‰; range 4–11 ‰) observed in the spectra of MT-SOA are also comparable to background $f_{82}^{OA}$ levels (average $4.3 \pm 0.9$ ‰; range 0.01–10 ‰), and tend to be in the higher $f_{82}^{OA}$ region from urban and biomass-burning emissions. A linear regression line of $f_{44}^{OA}$ vs. $f_{82}^{OA}$ for the Rocky Mountain site ($f_{82}^{OA} = 7.7 \times 10^{-3} - 0.019 \times f_{44}^{OA}$) is used to estimate the background $f_{82}^{OA}$ from areas strongly influenced by monoterpene emissions.

In summary, elevated $f_{82}^{OA}$ in studies with high isoprene emissions is observed. Pronounced $f_{82}^{IEPOX\text{-}SOA}$ should be a key feature of IEPOX-SOA spectra. Thus, IEPOX-SOA can be estimated as Eq. (A1)

$$\begin{aligned} \text{IEPOX-SOA} &= \frac{\text{m82}_{\text{total}} - \text{m82}_{\text{background}}}{f_{82}^{IEPOX\text{-}SOA} - f_{82}^{OA\text{-}Bkg}} \\ &= \frac{\text{m82}_{\text{total}} - \text{OA}_{\text{mass}} \times f_{82}^{OA\text{-}Bkg}}{f_{82}^{IEPOX\text{-}SOA} - f_{82}^{OA\text{-}Bkg}}, \end{aligned} \quad \text{(A1)}$$

where $f_{82}^{IEPOX\text{-}SOA}$ is 22 ‰ as obtained average (Fig. A3). In Eq. (4), $f_{82}^{OA\text{-}Bkg}$ can be calculated as a function of $f_{44}^{OA}$ in studies strongly influenced by urban and biomass-burning emissions ($f_{82}^{OA} = 5.5 \times 10^{-3} - 8.2 \times 10^{-3} \times f_{44}^{OA}$) or monoterpene emissions ($f_{82}^{OA} = 7.7 \times 10^{-3} - 0.019 \times f_{44}^{OA}$), as discussed earlier. $\text{m82}_{\text{total}}$ and $\text{OA}_{\text{mass}}$ are the measured ambient $m/z$ 82 and OA mass concentrations by AMS. Because $f_{82}$ in MT-SOA and OA from urban and biomass-burning emissions cannot be separated, only one background value of $f_{82}^{OA\text{-}Bkg}$ will be used in the UMR method.

To test this UMR empirical method, we apply Eq. (A1) to SOAS-CTR data set; see Fig. A4. The estimated IEPOX-SOA in SOAS-CTR from both background corrections (urban + biomass burning vs. monoterpene) both correlates well with $\text{IEPOX-SOA}_{\text{PMF}}$ with $R = 0.97$ and $R = 0.98$, respectively. The regression slopes between estimated fresh IEPOX-SOA vs. $\text{IEPOX-SOA}_{\text{PMF}}$ are 1.11 and 0.94, which are within 15 % of 1 : 1 line. The deviation of estimated IEPOX-SOA from UMR by subtracting the background of MT-SOA influences is similar to that from HR in the SOAS data set, indicating the UMR-based IEPOX-SOA estimation may perform as well as HR in areas with high IEPOX-SOA fractions. For areas with small IEPOX-SOA fractions, more uncertainties may exist in UMR calculation; e.g., there are wider variations of $f_{82}^{OA\text{-}Bkg}$ from urban and biomass-burning emissions with oxidation level, whereas a smaller and less variable $f_{C_5H_6O}^{OA\text{-}Bkg}$ is found in HR. Overall, $m/z$ 82 in unit mass-resolution data is also useful to estimate IEPOX-SOA. The different methods to estimate IEPOX-SOA may perform less well because of increased interferences from other ions at $m/z$ 82; however, at locations with very high fractions of IEPOX-SOA such as SOAS-CTR, the UMR-based method performs well.

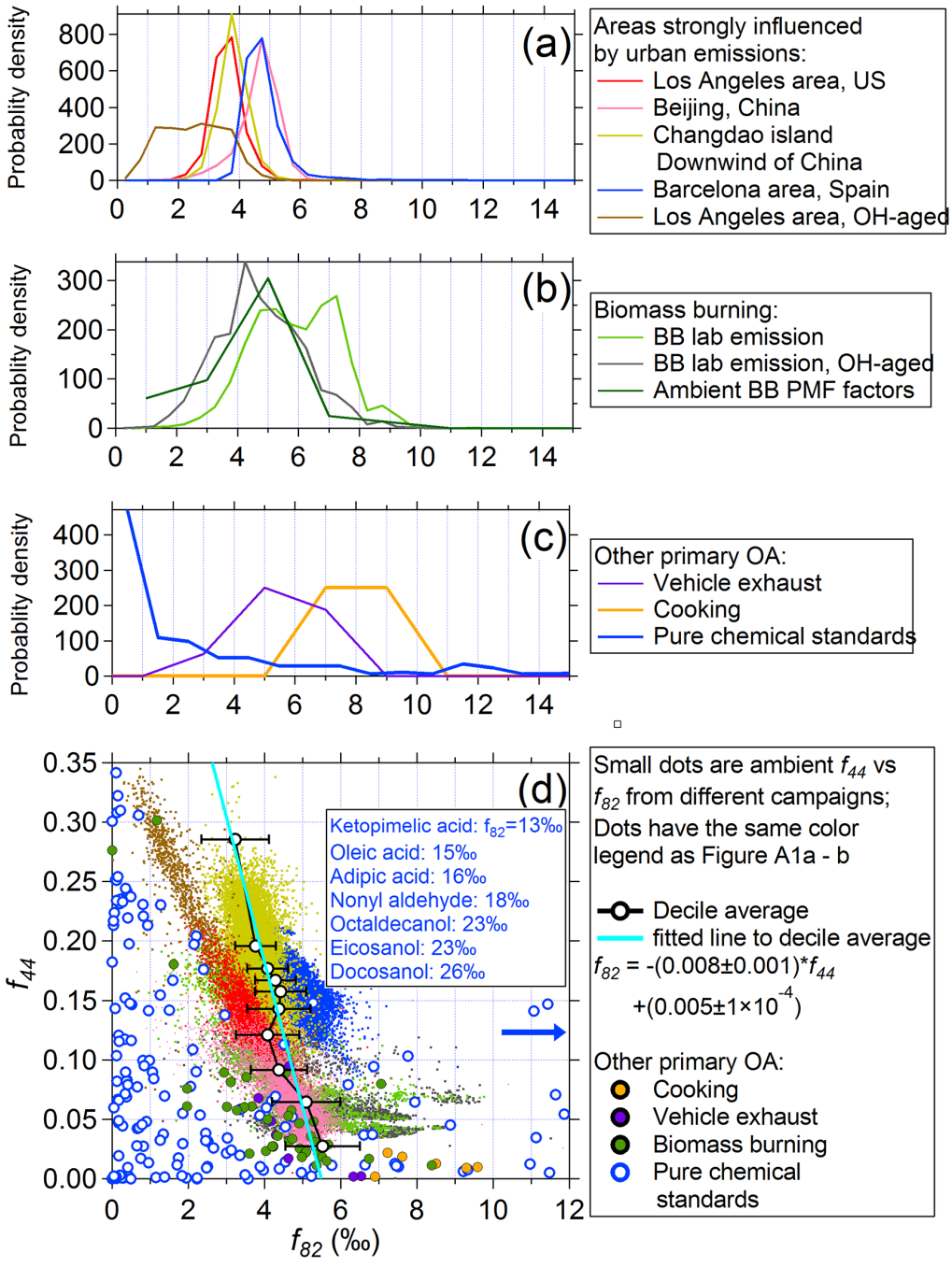


**Figure A1.** Probability density distributions of $f_{82}$ in studies **(a)** strongly influenced by urban emissions, **(b)** biomass-burning emissions, **(c)** other anthropogenic primary OA sources and pure chemical standards. Several pure chemical species showing higher $f_{82}$ between 15 and 30 ‰ are labeled with arrow. **(d)** Scatter plot of $f_{44}$ ($f_{44} = m/z$ 44/OA) vs. $f_{82}$ for all studies shown in panels **(a)**–**(c)**, using the same color scheme. Quantile averages of $f_{82}$ across all studies sorted by $f_{44}$ are also shown, as is a linear regression line to the quantile points.

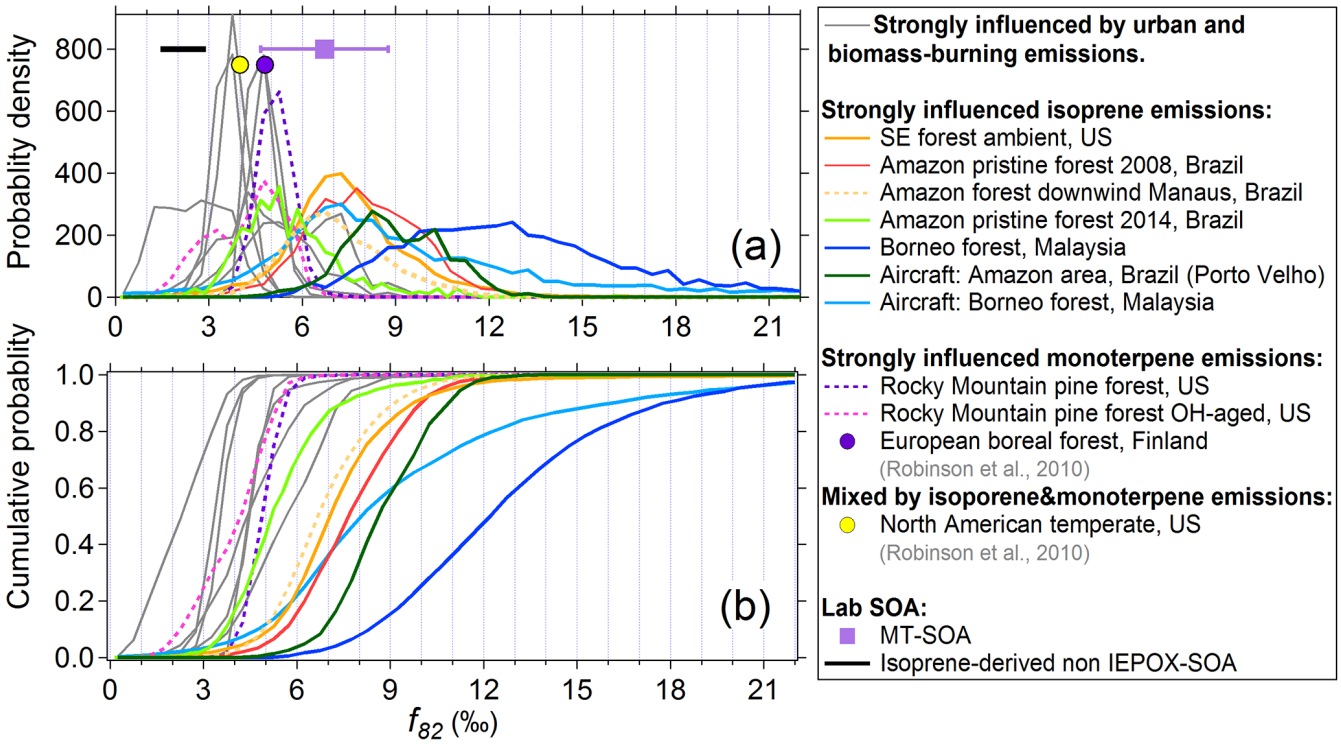


**Figure A2. (a)** Probability density and **(b)** cumulative probability distributions of $f_{82}$ in studies strongly influenced by isoprene and/or monoterpene emissions. The ranges of $f_{82}$ from other non-IEPOX-derived isoprene-SOA and MT-SOA are also shown. The background grey lines are from studies strongly influenced by urban and biomass-burning emissions and are the same data from Fig. A1a–b.

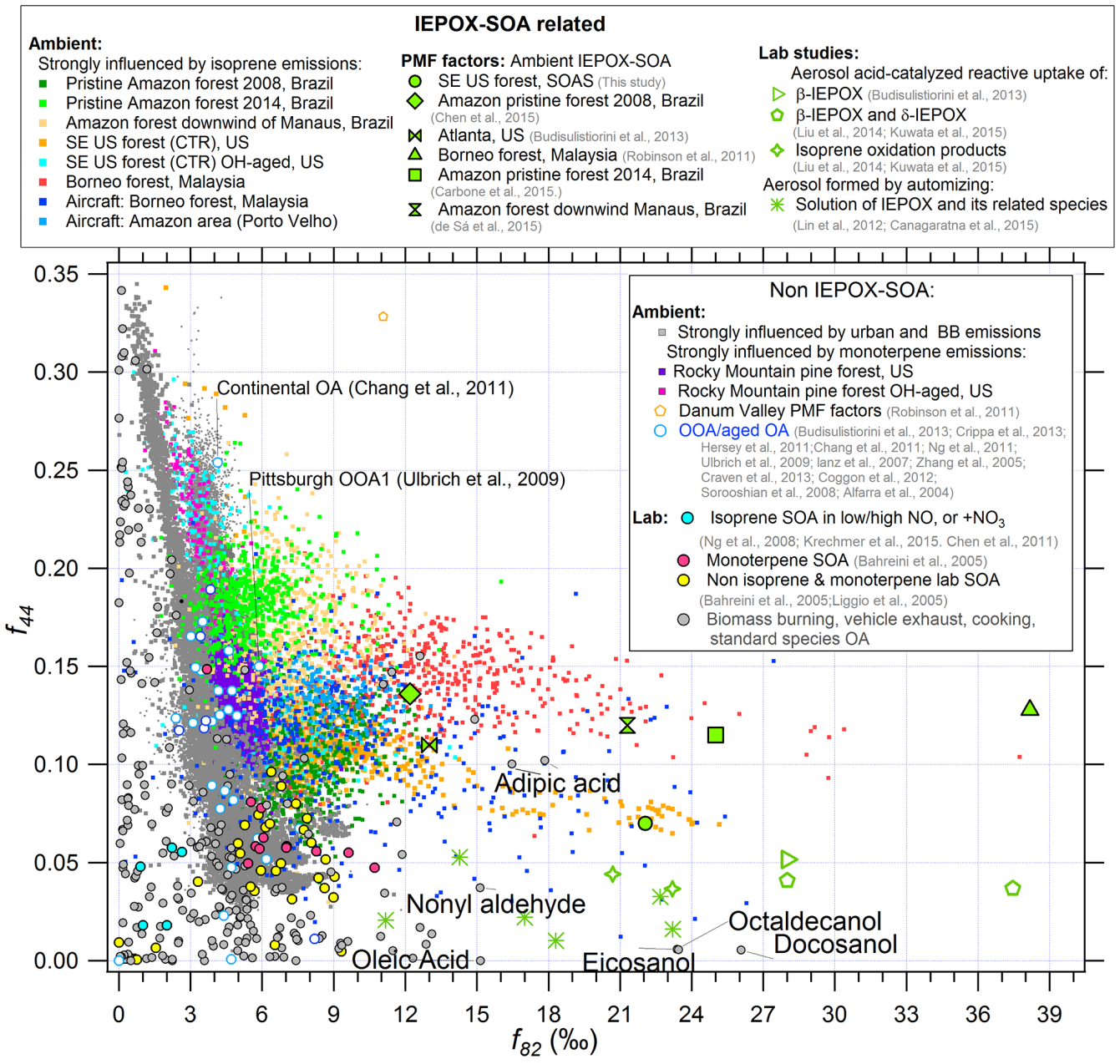


**Figure A3.** Scatter plot of $f_{44}$ and $f_{82}$ in studies strongly by isoprene and monoterpene emissions, as well as other OA sources. The grey dots represent background levels from studies strongly influenced by urban and biomass-burning emissions in Fig. A1d. $f_{44}$ and $f_{82}$ values from multiple sources of OA (Jimenez-Group, 2015) are also shown, together with IEPOX-SOA from different ambient PMF factors and chamber studies.

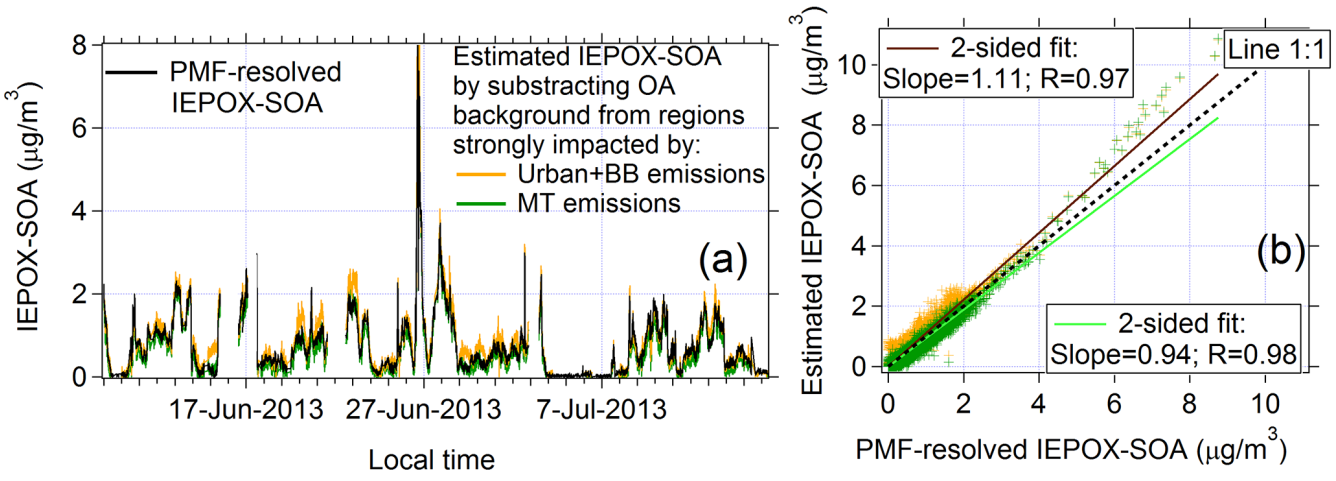


**Figure A4. (a)** Time series of IEPOX-SOA$_{PMF}$ and estimated IEPOX-SOA based on $m/z$ 82 for the SOAS-CTR data in SE US forest. Two different estimates of background $m/z$ 82 are shown, using values from regions strongly impacted by urban and biomass-burning emissions vs. regions with strong monoterpene emissions. **(b)** Scatter plot of estimated IEPOX-SOA vs. IEPOX-SOA$_{PMF}$. Note that the largest IEPOX-SOA plume ($> 4\,\mu g\,m^{-3}$) on 26 June 2013 had a slightly higher $f_{82}^{OA}$ of 24 ‰, resulting in a slight overestimation of IEPOX-SOA for those data points.

**The Supplement related to this article is available online at doi:10.5194/acp-15-11807-2015-supplement.**

*Acknowledgements.* This study was partially supported by NSF AGS-1243354 and AGS-1360834, NASA NNX12AC03G, DOE (BER/ASR) DE-SC0011105, and NOAA NA13OAR4310063. B. Palm and J. Krechmer are grateful for fellowships from EPA STAR (FP-91761701-0 and FP-91770901-0) and CIRES. A. Ortega is grateful for a CU-Boulder Chancellor's and DOE SCGF (ORAU/ORISE) fellowship. A. Wisthaler and T. Mikoviny were supported by the Austrian Federal Ministry for Transport, Innovation and Technology (BMVIT) through the Austrian Space Applications Programme (ASAP) of the Austrian Research Promotion Agency (FFG), and the Visiting Scientist Program at the National Institute of Aerospace (NIA). G. Isaacman-VanWertz is grateful for an NSF Fellowship (DGE-1106400). U. C. Berkeley was supported by NSF AGS-1250569. We acknowledge the logistical support from the LBA Central Office at INPA (Instituto Nacional de Pesquisas da Amazonia). P. Artaxo acknowledges support from FAPESP grants 2013/05014-0 and 2014/05238-8 and CNPq support from grants 457843/2013-6 and 307160/2014-9. We acknowledges this work was funded by the US Environmental Protection Agency (EPA) through grant number 835404. The contents of this publication are solely the responsibility of the authors and do not necessarily represent the official views of the US EPA. Further, the US EPA does not endorse the purchase of any commercial products or services mentioned in the publication. The US EPA through its Office of Research and Development collaborated in the research described here. It has been subjected to agency review and approved for publication, but may not necessarily reflect social agency policy. The authors would also like to thank the Electric Power Research Institute (EPRI) for their support. M. Riva and J. D. Surratt wish to thank the Camille and Henry Dreyfus Postdoctoral Fellowship Program in Environmental Chemistry for their financial support. We thank J. Crounse and P. Wennberg from Caltech for gas-phase IEPOX data in SOAS-CTR and DC3, under support from NASA NNX12AC06G. We thank Lu Xu and Nga Lee Ng from Georgia Tech for providing data from their studies. We acknowledge funding from the UK Natural Environment Research Council through the OP3 and SAMBBA projects (grant refs. NE/D002117/1 and NE/J010073/1).

Edited by: A. Carlton

## References

Aiken, A. C., Salcedo, D., Cubison, M. J., Huffman, J. A., DeCarlo, P. F., Ulbrich, I. M., Docherty, K. S., Sueper, D., Kimmel, J. R., Worsnop, D. R., Trimborn, A., Northway, M., Stone, E. A., Schauer, J. J., Volkamer, R. M., Fortner, E., de Foy, B., Wang, J., Laskin, A., Shutthanandan, V., Zheng, J., Zhang, R., Gaffney, J., Marley, N. A., Paredes-Miranda, G., Arnott, W. P., Molina, L. T., Sosa, G., and Jimenez, J. L.: Mexico City aerosol analysis during MILAGRO using high resolution aerosol mass spectrometry at the urban supersite (T0) – Part 1: Fine particle composition and organic source apportionment, Atmos. Chem. Phys., 9, 6633–6653, doi:10.5194/acp-9-6633-2009, 2009.

Alfarra, M.: Insights Into Atmospheric Organic Aerosols Using An Aerosol Mass Spectrometer, Doctor, Institute of Science and Technology, University of Manchester, Manchester, 2004.

Alfarra, M. R., Coe, H., Allan, J. D., Bower, K. N., Boudries, H., Canagaratna, M. R., Jimenez, J. L., Jayne, J. T., Garforth, A. A., Li, S. M., and Worsnop, D. R.: Characterization of urban and rural organic particulate in the lower Fraser valley using two aerodyne aerosol mass spectrometers, Atmos. Environ., 38, 5745–5758, doi:10.1016/j.atmosenv.2004.01.054, 2004.

Allan, J. D., Morgan, W. T., Darbyshire, E., Flynn, M. J., Williams, P. I., Oram, D. E., Artaxo, P., Brito, J., Lee, J. D., and Coe, H.: Airborne observations of IEPOX-derived isoprene SOA in the Amazon during SAMBBA, Atmos. Chem. Phys., 14, 11393–11407, doi:10.5194/acp-14-11393-2014, 2014.

Anonymous Referee: Interactive comment on "Airborne observations of IEPOX-derived isoprene SOA in the Amazon during SAMBBA" by J. D. Allan et al., Atmos. Chem. Phys. Discuss, 14, C5277–C5279, 2014.

Atkinson, R. and Arey, J.: Atmospheric Degradation of Volatile Organic Compounds, Chem. Rev., 103, 4605–4638, doi:10.1002/chin.200410285, 2003.

Bahreini, R., Keywood, M. D., Ng, N. L., Varutbangkul, V., Gao, S., Flagan, R. C., Seinfeld, J. H., Worsnop, D. R., and Jimenez, J. L.: Measurements of secondary organic aerosol from oxidation of cycloalkenes, terpenes, and m-xylene using an Aerodyne aerosol mass spectrometer, Environ. Sci. Technol., 39, 5674–5688, doi:10.1021/Es048061a, 2005.

Barth, M. C., Cantrell, C. A., Brune, W. H., Rutledge, S. A., Crawford, J. H., Huntrieser, H., Carey, L. D., MacGorman, D., Weisman, M., Pickering, K. E., Bruning, E., Anderson, B., Apel, E., Biggerstaff, M., Campos, T., Campuzano-Jost, P., Cohen, R., Crounse, J., Day, D. A., Diskin, G., Flocke, F., Fried, A., Garland, C., Heikes, B., Honomichl, S., Hornbrook, R., Huey, L. G., Jimenez, J. L., Lang, T., Lichtenstern, M., Mikoviny, T., Nault, B., O'Sullivan, D., Pan, L. L., Peischl, J., Pollack, I., Richter, D., Riemer, D., Ryerson, T., Schlager, H., Clair, J. S., Walega, J., Weibring, P., Weinheimer, A., Wennberg, P., Wisthaler, A., Wooldridge, P. J., and Ziegler, C.: The Deep Convective Clouds and Chemistry (DC3) Field Campaign, B. Am. Meteorol. Soc., 96, 1281–1309, doi:10.1175/bams-d-13-00290.1, 2015.

Boyd, C. M., Sanchez, J., Xu, L., Eugene, A. J., Nah, T., Tuet, W. Y., Guzman, M. I., and Ng, N. L.: Secondary organic aerosol formation from the $\beta$-pinene + $NO_3$ system: effect of humidity and peroxy radical fate, Atmos. Chem. Phys., 15, 7497–7522, doi:10.5194/acp-15-7497-2015, 2015.

Budisulistiorini, S. H., Canagaratna, M. R., Croteau, P. L., Marth, W. J., Baumann, K., Edgerton, E. S., Shaw, S. L., Knipping, E. M., Worsnop, D. R., Jayne, J. T., Gold, A., and Surratt, J. D.: Real-Time Continuous Characterization of Secondary Organic Aerosol Derived from Isoprene Epoxydiols in Downtown Atlanta, Georgia, Using the Aerodyne Aerosol Chemical Speciation Monitor, Environ. Sci. Technol., 47, 5686–5694, doi:10.1021/es400023n, 2013.

Budisulistiorini, S. H., Li, X., Bairai, S. T., Renfro, J., Liu, Y., Liu, Y. J., McKinney, K. A., Martin, S. T., McNeill, V. F., Pye, H. O. T., Nenes, A., Neff, M. E., Stone, E. A., Mueller, S., Knote, C., Shaw, S. L., Zhang, Z., Gold, A., and Surratt, J. D.:

Examining the effects of anthropogenic emissions on isoprene-derived secondary organic aerosol formation during the 2013 Southern Oxidant and Aerosol Study (SOAS) at the Look Rock, Tennessee ground site, Atmos. Chem. Phys., 15, 8871–8888, doi:10.5194/acp-15-8871-2015, 2015.

Canagaratna, M. R., Jayne, J. T., Ghertner, D. A., Herndon, S., Shi, Q., Jimenez, J. L., Silva, P. J., Williams, P., Lanni, T., Drewnick, F., Demerjian, K. L., Kolb, C. E., and Worsnop, D. R.: Chase studies of particulate emissions from in-use New York City vehicles, Aerosol. Sci. Tech., 38, 555–573, doi:10.1080/02786820490465504, 2004.

Canagaratna, M. R., Jimenez, J. L., Kroll, J. H., Chen, Q., Kessler, S. H., Massoli, P., Hildebrandt Ruiz, L., Fortner, E., Williams, L. R., Wilson, K. R., Surratt, J. D., Donahue, N. M., Jayne, J. T., and Worsnop, D. R.: Elemental ratio measurements of organic compounds using aerosol mass spectrometry: characterization, improved calibration, and implications, Atmos. Chem. Phys., 15, 253–272, doi:10.5194/acp-15-253-2015, 2015.

Carbone, S., De Brito, J. F., Andreae, M., Pöhlker, C., Chi, X., Saturno, J., Barbosa, H., and Artaxo, P.: Preliminary characterization of submicron secondary aerosol in the amazon forest – ATTO station, in preparation, 2015.

Chang, R. Y.-W., Leck, C., Graus, M., Müller, M., Paatero, J., Burkhart, J. F., Stohl, A., Orr, L. H., Hayden, K., Li, S.-M., Hansel, A., Tjernström, M., Leaitch, W. R., and Abbatt, J. P. D.: Aerosol composition and sources in the central Arctic Ocean during ASCOS, Atmos. Chem. Phys., 11, 10619–10636, doi:10.5194/acp-11-10619-2011, 2011.

Chen, Q., Liu, Y., Donahue, N. M., Shilling, J. E., and Martin, S. T.: Particle-Phase Chemistry of Secondary Organic Material: Modeled Compared to Measured O : C and H : C Elemental Ratios Provide Constraints, Environ. Sci. Technol., 45, 4763–4770, doi:10.1021/es104398s, 2011.

Chen, Q., Farmer, D. K., Rizzo, L. V., Pauliquevis, T., Kuwata, M., Karl, T. G., Guenther, A., Allan, J. D., Coe, H., Andreae, M. O., Pöschl, U., Jimenez, J. L., Artaxo, P., and Martin, S. T.: Submicron particle mass concentrations and sources in the Amazonian wet season (AMAZE-08), Atmos. Chem. Phys., 15, 3687–3701, doi:10.5194/acp-15-3687-2015, 2015.

Chhabra, P. S., Ng, N. L., Canagaratna, M. R., Corrigan, A. L., Russell, L. M., Worsnop, D. R., Flagan, R. C., and Seinfeld, J. H.: Elemental composition and oxidation of chamber organic aerosol, Atmos. Chem. Phys., 11, 8827–8845, doi:10.5194/acp-11-8827-2011, 2011.

Coggon, M. M., Sorooshian, A., Wang, Z., Metcalf, A. R., Frossard, A. A., Lin, J. J., Craven, J. S., Nenes, A., Jonsson, H. H., Russell, L. M., Flagan, R. C., and Seinfeld, J. H.: Ship impacts on the marine atmosphere: insights into the contribution of shipping emissions to the properties of marine aerosol and clouds, Atmos. Chem. Phys., 12, 8439–8458, doi:10.5194/acp-12-8439-2012, 2012.

Cole-Filipiak, N. C., O'Connor, A. E., and Elrod, M. J.: Kinetics of the Hydrolysis of Atmospherically Relevant Isoprene-Derived Hydroxy Epoxides, Environ. Sci. Technol., 44, 6718–6723, doi:10.1021/es1019228, 2010.

Corrigan, A. L., Russell, L. M., Takahama, S., Äijälä, M., Ehn, M., Junninen, H., Rinne, J., Petäjä, T., Kulmala, M., Vogel, A. L., Hoffmann, T., Ebben, C. J., Geiger, F. M., Chhabra, P., Seinfeld, J. H., Worsnop, D. R., Song, W., Auld, J., and Williams, J.: Biogenic and biomass burning organic aerosol in a boreal forest at Hyytiälä, Finland, during HUMPPA-COPEC 2010, Atmos. Chem. Phys., 13, 12233–12256, doi:10.5194/acp-13-12233-2013, 2013.

Crippa, M., El Haddad, I., Slowik, J. G., DeCarlo, P. F., Mohr, C., Heringa, M. F., Chirico, R., Marchand, N., Sciare, J., Baltensperger, U., and Prévôt, A. S. H.: Identification of marine and continental aerosol sources in Paris using high resolution aerosol mass spectrometry, J. Geophys. Res.-Atmos., 118, 1950–1963, doi:10.1002/jgrd.50151, 2013.

Cubison, M. J., Ortega, A. M., Hayes, P. L., Farmer, D. K., Day, D., Lechner, M. J., Brune, W. H., Apel, E., Diskin, G. S., Fisher, J. A., Fuelberg, H. E., Hecobian, A., Knapp, D. J., Mikoviny, T., Riemer, D., Sachse, G. W., Sessions, W., Weber, R. J., Weinheimer, A. J., Wisthaler, A., and Jimenez, J. L.: Effects of aging on organic aerosol from open biomass burning smoke in aircraft and laboratory studies, Atmos. Chem. Phys., 11, 12049–12064, doi:10.5194/acp-11-12049-2011, 2011.

DeCarlo, P. F., Kimmel, J. R., Trimborn, A., Northway, M. J., Jayne, J. T., Aiken, A. C., Gonin, M., Fuhrer, K., Horvath, T., Docherty, K. S., Worsnop, D. R., and Jimenez, J. L.: Field-deployable, high-resolution, time-of-flight aerosol mass spectrometer, Anal. Chem., 78, 8281–8289, doi:10.1021/Ac061249n, 2006.

de Sá, S. S., Palm, B. B., Campuzano-Jost, P., Day, D. A., Hu, W., Newburn, M. K., Brito, J., Liu, Y., Isaacman-VanWertz, G., Yee, L. D., Goldstein, A. H., Artaxo, P., Souza, R., Manzi, A., Jimenez, J. L., Alexander, M. L., and Martin, S. T.:, in preparation, 2015.

Docherty, K. S., Aiken, A. C., Huffman, J. A., Ulbrich, I. M., DeCarlo, P. F., Sueper, D., Worsnop, D. R., Snyder, D. C., Peltier, R. E., Weber, R. J., Grover, B. D., Eatough, D. J., Williams, B. J., Goldstein, A. H., Ziemann, P. J., and Jimenez, J. L.: The 2005 Study of Organic Aerosols at Riverside (SOAR-1): instrumental intercomparisons and fine particle composition, Atmos. Chem. Phys., 11, 12387–12420, doi:10.5194/acp-11-12387-2011, 2011.

Dunlea, E. J., DeCarlo, P. F., Aiken, A. C., Kimmel, J. R., Peltier, R. E., Weber, R. J., Tomlinson, J., Collins, D. R., Shinozuka, Y., McNaughton, C. S., Howell, S. G., Clarke, A. D., Emmons, L. K., Apel, E. C., Pfister, G. G., van Donkelaar, A., Martin, R. V., Millet, D. B., Heald, C. L., and Jimenez, J. L.: Evolution of Asian aerosols during transpacific transport in INTEX-B, Atmos. Chem. Phys., 9, 7257–7287, doi:10.5194/acp-9-7257-2009, 2009.

Dzepina, K., Arey, J., Marr, L. C., Worsnop, D. R., Salcedo, D., Zhang, Q., Onasch, T. B., Molina, L. T., Molina, M. J., and Jimenez, J. L.: Detection of particle-phase polycyclic aromatic hydrocarbons in Mexico City using an aerosol mass spectrometer, Int. J. Mass Spectrom., 263, 152–170, doi:10.1016/j.ijms.2007.01.010, 2007.

Ebben, C. J., Martinez, I. S., Shrestha, M., Buchbinder, A. M., Corrigan, A. L., Guenther, A., Karl, T., Petäjä, T., Song, W. W., Zorn, S. R., Artaxo, P., Kulmala, M., Martin, S. T., Russell, L. M., Williams, J., and Geiger, F. M.: Contrasting organic aerosol particles from boreal and tropical forests during HUMPPA-COPEC-2010 and AMAZE-08 using coherent vibrational spectroscopy, Atmos. Chem. Phys., 11, 10317–10329, doi:10.5194/acp-11-10317-2011, 2011.

Eddingsaas, N. C., VanderVelde, D. G., and Wennberg, P. O.: Kinetics and Products of the Acid-Catalyzed Ring-Opening of At-

mospherically Relevant Butyl Epoxy Alcohols, J. Phys. Chem. A, 114, 8106–8113, doi:10.1021/jp103907c, 2010.

Fröhlich, R., Crenn, V., Setyan, A., Belis, C. A., Canonaco, F., Favez, O., Riffault, V., Slowik, J. G., Aas, W., Aijälä, M., Alastuey, A., Artiñano, B., Bonnaire, N., Bozzetti, C., Bressi, M., Carbone, C., Coz, E., Croteau, P. L., Cubison, M. J., Esser-Gietl, J. K., Green, D. C., Gros, V., Heikkinen, L., Herrmann, H., Jayne, J. T., Lunder, C. R., Minguillón, M. C., Mocnik, G., O'Dowd, C. D., Ovadnevaite, J., Petralia, E., Poulain, L., Priestman, M., Ripoll, A., Sarda-Estève, R., Wiedensohler, A., Baltensperger, U., Sciare, J., and Prévôt, A. S. H.: ACTRIS ACSM intercomparison – Part 2: Intercomparison of ME-2 organic source apportionment results from 15 individual, co-located aerosol mass spectrometers, Atmos. Meas. Tech., 8, 2555–2576, doi:10.5194/amt-8-2555-2015, 2015.

Froyd, K. D., Murphy, S. M., Murphy, D. M., de Gouw, J. A., Eddingsaas, N. C., and Wennberg, P. O.: Contribution of isoprene-derived organosulfates to free tropospheric aerosol mass, P. Natl. Acad. Sci. USA, 107, 21360–21365, doi:10.1073/pnas.1012561107, 2010.

Fry, J. L., Draper, D. C., Zarzana, K. J., Campuzano-Jost, P., Day, D. A., Jimenez, J. L., Brown, S. S., Cohen, R. C., Kaser, L., Hansel, A., Cappellin, L., Karl, T., Hodzic Roux, A., Turnipseed, A., Cantrell, C., Lefer, B. L., and Grossberg, N.: Observations of gas- and aerosol-phase organic nitrates at BEACHON-RoMBAS 2011, Atmos. Chem. Phys., 13, 8585–8605, doi:10.5194/acp-13-8585-2013, 2013.

Fry, J. L., Draper, D. C., Barsanti, K. C., Smith, J. N., Ortega, J., Winkler, P. M., Lawler, M. J., Brown, S. S., Edwards, P. M., Cohen, R. C., and Lee, L.: Secondary Organic Aerosol Formation and Organic Nitrate Yield from $NO_3$ Oxidation of Biogenic Hydrocarbons, Environ. Sci. Technol, 48, 11944–11953, doi:10.1021/es502204x, 2014.

Gaston, C. J., Riedel, T. P., Zhang, Z., Gold, A., Surratt, J. D., and Thornton, J. A.: Reactive Uptake of an Isoprene-Derived Epoxydiol to Submicron Aerosol Particles, Environ. Sci. Technol., 48, 11178–11186, doi:10.1021/es5034266, 2014.

Guenther, A. B., Jiang, X., Heald, C. L., Sakulyanontvittaya, T., Duhl, T., Emmons, L. K., and Wang, X.: The Model of Emissions of Gases and Aerosols from Nature version 2.1 (MEGAN2.1): an extended and updated framework for modeling biogenic emissions, Geosci. Model Dev., 5, 1471–1492, doi:10.5194/gmd-5-1471-2012, 2012.

Hayes, P. L., Ortega, A. M., Cubison, M. J., Froyd, K. D., Zhao, Y., Cliff, S. S., Hu, W. W., Toohey, D. W., Flynn, J. H., Lefer, B. L., Grossberg, N., Alvarez, S., Rappenglück, B., Taylor, J. W., Allan, J. D., Holloway, J. S., Gilman, J. B., Kuster, W. C., de Gouw, J. A., Massoli, P., Zhang, X., Liu, J., Weber, R. J., Corrigan, A. L., Russell, L. M., Isaacman, G., Worton, D. R., Kreisberg, N. M., Goldstein, A. H., Thalman, R., Waxman, E. M., Volkamer, R., Lin, Y. H., Surratt, J. D., Kleindienst, T. E., Offenberg, J. H., Dusanter, S., Griffith, S., Stevens, P. S., Brioude, J., Angevine, W. M., and Jimenez, J. L.: Organic aerosol composition and sources in Pasadena, California, during the 2010 CalNex campaign, J. Geophys. Res.-Atmos., 118, 9233–9257, doi:10.1002/jgrd.50530, 2013.

He, L.-Y., Lin, Y., Huang, X.-F., Guo, S., Xue, L., Su, Q., Hu, M., Luan, S.-J., and Zhang, Y.-H.: Characterization of high-resolution aerosol mass spectra of primary organic aerosol emissions from Chinese cooking and biomass burning, Atmos. Chem. Phys., 10, 11535–11543, doi:10.5194/acp-10-11535-2010, 2010.

Hersey, S. P., Craven, J. S., Schilling, K. A., Metcalf, A. R., Sorooshian, A., Chan, M. N., Flagan, R. C., and Seinfeld, J. H.: The Pasadena Aerosol Characterization Observatory (PACO): chemical and physical analysis of the Western Los Angeles basin aerosol, Atmos. Chem. Phys., 11, 7417–7443, doi:10.5194/acp-11-7417-2011, 2011.

Hu, D., Bian, Q., Li, T. W. Y., Lau, A. K. H., and Yu, J. Z.: Contributions of isoprene, monoterpenes, $\beta$-caryophyllene, and toluene to secondary organic aerosols in Hong Kong during the summer of 2006, J. Geophys. Res.-Atmos., 113, D22206, doi:10.1029/2008jd010437, 2008.

Hu, W., Hu, M., Hu, W., Jimenez, J.-L., Yuan, B., Chen, W., Wang, M., Wu, Y., Wang, Z., Chen, C., Peng, J., Shao, M., and Zeng, L.: Chemical composition, sources and aging process of sub-micron aerosols in Beijing: contrast between summer and winter, J. Geophys. Res.-Atmos., in review, 2015.

Hu, W. W., Hu, M., Yuan, B., Jimenez, J. L., Tang, Q., Peng, J. F., Hu, W., Shao, M., Wang, M., Zeng, L. M., Wu, Y. S., Gong, Z. H., Huang, X. F., and He, L. Y.: Insights on organic aerosol aging and the influence of coal combustion at a regional receptor site of central eastern China, Atmos. Chem. Phys., 13, 10095–10112, doi:10.5194/acp-13-10095-2013, 2013.

Huang, X.-F., He, L.-Y., Hu, M., Canagaratna, M. R., Sun, Y., Zhang, Q., Zhu, T., Xue, L., Zeng, L.-W., Liu, X.-G., Zhang, Y.-H., Jayne, J. T., Ng, N. L., and Worsnop, D. R.: Highly time-resolved chemical characterization of atmospheric submicron particles during 2008 Beijing Olympic Games using an Aerodyne High-Resolution Aerosol Mass Spectrometer, Atmos. Chem. Phys., 10, 8933–8945, doi:10.5194/acp-10-8933-2010, 2010.

Isaacman, G., Kreisberg, N. M., Yee, L. D., Worton, D. R., Chan, A. W. H., Moss, J. A., Hering, S. V., and Goldstein, A. H.: Online derivatization for hourly measurements of gas- and particle-phase semi-volatile oxygenated organic compounds by thermal desorption aerosol gas chromatography (SV-TAG), Atmos. Meas. Tech., 7, 4417–4429, doi:10.5194/amt-7-4417-2014, 2014.

Jacobs, M. I., Burke, W. J., and Elrod, M. J.: Kinetics of the reactions of isoprene-derived hydroxynitrates: gas phase epoxide formation and solution phase hydrolysis, Atmos. Chem. Phys., 14, 8933–8946, doi:10.5194/acp-14-8933-2014, 2014.

Jimenez-Group: Aerosol Mass Spectrometer Web Mass Spectral Database, High-Resolution AMS Spectra, available at: http://cires.colorado.edu/jimenez-group/HRAMSsd/ (last access: 15 December 2014); unit mass resolution spectra, available at: http://cires1.colorado.edu/jimenez-group/AMSsd/ (last access: 15 December 2014), University of Colorado, Boulder, 2015.

Jimenez, J. L., Jayne, J. T., Shi, Q., Kolb, C. E., Worsnop, D. R., Yourshaw, I., Seinfeld, J. H., Flagan, R. C., Zhang, X. F., Smith, K. A., Morris, J. W., and Davidovits, P.: Ambient aerosol sampling using the Aerodyne Aerosol Mass Spectrometer, J. Geophys. Res.-Atmos., 108, 8425, doi:10.1029/2001jd001213, 2003.

Kang, E., Root, M. J., Toohey, D. W., and Brune, W. H.: Introducing the concept of Potential Aerosol Mass (PAM), Atmos. Chem. Phys., 7, 5727–5744, doi:10.5194/acp-7-5727-2007, 2007.

Karl, T., Guenther, A., Turnipseed, A., Tyndall, G., Artaxo, P., and Martin, S.: Rapid formation of isoprene photo-oxidation products observed in Amazonia, Atmos. Chem. Phys., 9, 7753–7767, doi:10.5194/acp-9-7753-2009, 2009.

Karl, T., Kaser, L., and Turnipseed, A.: Eddy covariance measurements of isoprene and 232-MBO based on NO+ time-of-flight mass spectrometry, Int. J. Mass Spectrom., 365–366, 15-19, 2014.

Kaser, L., Karl, T., Schnitzhofer, R., Graus, M., Herdlinger-Blatt, I. S., DiGangi, J. P., Sive, B., Turnipseed, A., Hornbrook, R. S., Zheng, W., Flocke, F. M., Guenther, A., Keutsch, F. N., Apel, E., and Hansel, A.: Comparison of different real time VOC measurement techniques in a ponderosa pine forest, Atmos. Chem. Phys., 13, 2893–2906, 10, http://www.atmos-chem-phys.net/13/2893/10/.5194/acp-13-2893-2013, 2013.

Katrib, Y., Martin, S. T., Hung, H.-M., Rudich, Y., Zhang, H., Slowik, J. G., Davidovits, P., Jayne, J. T., and Worsnop, D. R.: Products and Mechanisms of Ozone Reactions with Oleic Acid for Aerosol Particles Having Core–Shell Morphologies, J. Phys. Chem. A, 108, 6686–6695, doi:10.1021/jp049759d, 2004.

Krechmer, J. E., Coggon, M. M., Massoli, P., Nguyen, T. B., Crounse, J. D., Hu, W., Day, D. A., Tyndall, G. S., Henze, D. K., Rivera-Rios, J. C., Nowak, J. B., Kimmel, J. R., Mauldin, R. L., Stark, H., Jayne, J. T., Sipilä, M., Junninen, H., St. Clair, J. M., Zhang, X., Feiner, P. A., Zhang, L., Miller, D. O., Brune, W. H., Keutsch, F. N., Wennberg, P. O., Seinfeld, J. H., Worsnop, D. R., Jimenez, J. L., and Canagaratna, M. R.: Formation of Low Volatility Organic Compounds and Secondary Organic Aerosol from Isoprene Hydroxyhydroperoxide Low-NO Oxidation, Environ. Sci. Technol., 49, 10330–10339, doi:10.1021/acs.est.5b02031, 2015.

Kroll, J. H., Ng, N. L., Murphy, S. M., Flagan, R. C., and Seinfeld, J. H.: Secondary organic aerosol formation from isoprene photooxidation, Environ. Sci. Technol., 40, 1869–1877, doi:10.1021/Es0524301, 2006.

Kuwata, M., Liu, Y., McKinney, K., and Martin, S. T.: Physical state and acidity of inorganic sulfate can regulate the production of secondary organic material from isoprene photooxidation products, Phys. Chem. Chem. Phys., 17, 5670–5678, doi:10.1039/c4cp04942j, 2015.

Lanz, V. A., Alfarra, M. R., Baltensperger, U., Buchmann, B., Hueglin, C., and Prévôt, A. S. H.: Source apportionment of submicron organic aerosols at an urban site by factor analytical modelling of aerosol mass spectra, Atmos. Chem. Phys., 7, 1503–1522, doi:10.5194/acp-7-1503-2007, 2007.

Levin, E. J. T., Prenni, A. J., Palm, B. B., Day, D. A., Campuzano-Jost, P., Winkler, P. M., Kreidenweis, S. M., DeMott, P. J., Jimenez, J. L., and Smith, J. N.: Size-resolved aerosol composition and its link to hygroscopicity at a forested site in Colorado, Atmos. Chem. Phys., 14, 2657–2667, doi:10.5194/acp-14-2657-2014, 2014.

Lewandowski, M., Piletic, I. R., Kleindienst, T. E., Offenberg, J. H., Beaver, M. R., Jaoui, M., Docherty, K. S., and Edney, E. O.: Secondary organic aerosol characterisation at field sites across the United States during the spring–summer period, International Journal of Environmental Analytical Chemistry, 93, 1084–1103, doi:10.1080/03067319.2013.803545, 2013.

Li, R., Palm, B. B., Borbon, A., Graus, M., Warneke, C., Ortega, A. M., Day, D. A., Brune, W. H., Jimenez, J. L., and de Gouw, J. A.: Laboratory Studies on Secondary Organic Aerosol Formation from Crude Oil Vapors, Environ. Sci. Technol., 47, 12566–12574, doi:10.1021/es402265y, 2013.

Li, Y. J., Yeung, J. W. T., Leung, T. P. I., Lau, A. P. S., and Chan, C. K.: Characterization of Organic Particles from Incense Burning Using an Aerodyne High-Resolution Time-of-Flight Aerosol Mass Spectrometer, Aerosol. Sci. Tech., 46, 654–665, doi:10.1080/02786826.2011.653017, 2011.

Liao, J., Froyd, K. D., Murphy, D. M., Keutsch, F. N., Yu, G., Wennberg, P. O., Clair, J. S., Crounse, J. D., Wisthaler, A., Mikoviny, T., Ryerson, T. B., Pollack, I. B., Peischl, J. L., Collett, J., Jimenez, J. L., Campuzano-Jost, P., Day, D. A., Hu, W. W., Anderson, B. E., Ziemba, L. D., Blake, D. R., Meinardi, S., and Diskin, G.: Airborne organosulfates measurements over the continental US, J. Geophys. Res.-Atmos., 120, 2990–3005, 2014.

Liggio, J., Li, S. M., and Mclaren, R.: Reactive uptake of glyoxal by particulate matter, J. Geophys. Res.-Atmos., 110, D10304, doi:10.1029/2004jd005113, 2005.

Lin, Y.-H., Zhang, Z., Docherty, K. S., Zhang, H., Budisulistiorini, S. H., Rubitschun, C. L., Shaw, S. L., Knipping, E. M., Edgerton, E. S., Kleindienst, T. E., Gold, A., and Surratt, J. D.: Isoprene Epoxydiols as Precursors to Secondary Organic Aerosol Formation: Acid-Catalyzed Reactive Uptake Studies with Authentic Compounds, Environ. Sci. Technol., 46, 250–258, doi:10.1021/es202554c, 2012.

Lin, Y.-H., Budisulistiorini, S. H., Chu, K., Siejack, R. A., Zhang, H., Riva, M., Zhang, Z., Gold, A., Kautzman, K. E., and Surratt, J. D.: Light-Absorbing Oligomer Formation in Secondary Organic Aerosol from Reactive Uptake of Isoprene Epoxydiols, Environ. Sci. Technol., 48, 12012–12021, doi:10.1021/es503142b, 2014.

Liu, Y., Kuwata, M., Strick, B. F., Thomson, R. J., Geiger, F. M., McKinney, K., and Martin, S. T.: Uptake of Epoxydiol Isomers Accounts for Half of the Particle-Phase Material Produced from Isoprene Photooxidation via the $HO_2$ pathway, Environ. Sci. Technol., 49, 250–258, doi:10.1021/es5034298, 2014.

Loza, C. L., Chhabra, P. S., Yee, L. D., Craven, J. S., Flagan, R. C., and Seinfeld, J. H.: Chemical aging of m-xylene secondary organic aerosol: laboratory chamber study, Atmos. Chem. Phys., 12, 151–167, doi:10.5194/acp-12-151-2012, 2012.

Mael, L. E., Jacobs, M. I., and Elrod, M. J.: Organosulfate and Nitrate Formation and Reactivity from Epoxides Derived from 2-Methyl-3-buten-2-ol, J. Phys. Chem. A, 119, 4464–4472, doi:10.1021/jp510033s, 2014.

Mao, J., Paulot, F., Jacob, D. J., Cohen, R. C., Crounse, J. D., Wennberg, P. O., Keller, C. A., Hudman, R. C., Barkley, M. P., and Horowitz, L. W.: Ozone and organic nitrates over the eastern United States: Sensitivity to isoprene chemistry, J. Geophys. Res.-Atmos., 118, 2013JD020231, doi:10.1002/jgrd.50817, 2013.

Middlebrook, A. M., Bahreini, R., Jimenez, J. L., and Canagaratna, M. R.: Evaluation of Composition-Dependent Collection Efficiencies for the Aerodyne Aerosol Mass Spectrometer using Field Data, Aerosol Sci. Tech., 46, 258–271, doi:10.1080/02786826.2011.620041, 2012.

Minguillón, M. C., Perron, N., Querol, X., Szidat, S., Fahrni, S. M., Alastuey, A., Jimenez, J. L., Mohr, C., Ortega, A. M., Day,

D. A., Lanz, V. A., Wacker, L., Reche, C., Cusack, M., Amato, F., Kiss, G., Hoffer, A., Decesari, S., Moretti, F., Hillamo, R., Teinilä, K., Seco, R., Peñuelas, J., Metzger, A., Schallhart, S., Müller, M., Hansel, A., Burkhart, J. F., Baltensperger, U., and Prévôt, A. S. H.: Fossil versus contemporary sources of fine elemental and organic carbonaceous particulate matter during the DAURE campaign in Northeast Spain, Atmos. Chem. Phys., 11, 12067–12084, doi:10.5194/acp-11-12067-2011, 2011.

Mohr, C., Huffman, J. A., Cubison, M. J., Aiken, A. C., Docherty, K. S., Kimmel, J. R., Ulbricht, I. M., Hannigan, M., and Jimenez, J. L.: Characterization of Primary Organic Aerosol Emissions from Meat Cooking, Trash Burning, and Motor Vehicles with High-Resolution Aerosol Mass Spectrometry and Comparison with Ambient and Chamber Observations, Environ. Sci. Technol., 43, 2443–2449, doi:10.1021/Es8011518, 2009.

Mohr, C., DeCarlo, P. F., Heringa, M. F., Chirico, R., Slowik, J. G., Richter, R., Reche, C., Alastuey, A., Querol, X., Seco, R., Peñuelas, J., Jiménez, J. L., Crippa, M., Zimmermann, R., Baltensperger, U., and Prévôt, A. S. H.: Identification and quantification of organic aerosol from cooking and other sources in Barcelona using aerosol mass spectrometer data, Atmos. Chem. Phys., 12, 1649–1665, doi:10.5194/acp-12-1649-2012, 2012.

Ng, N. L., Chhabra, P. S., Chan, A. W. H., Surratt, J. D., Kroll, J. H., Kwan, A. J., McCabe, D. C., Wennberg, P. O., Sorooshian, A., Murphy, S. M., Dalleska, N. F., Flagan, R. C., and Seinfeld, J. H.: Effect of $NO_x$ level on secondary organic aerosol (SOA) formation from the photooxidation of terpenes, Atmos. Chem. Phys., 7, 5159–5174, doi:10.5194/acp-7-5159-2007, 2007.

Ng, N. L., Kwan, A. J., Surratt, J. D., Chan, A. W. H., Chhabra, P. S., Sorooshian, A., Pye, H. O. T., Crounse, J. D., Wennberg, P. O., Flagan, R. C., and Seinfeld, J. H.: Secondary organic aerosol (SOA) formation from reaction of isoprene with nitrate radicals ($NO_3$), Atmos. Chem. Phys., 8, 4117–4140, doi:10.5194/acp-8-4117-2008, 2008.

Ng, N. L., Canagaratna, M. R., Jimenez, J. L., Chhabra, P. S., Seinfeld, J. H., and Worsnop, D. R.: Changes in organic aerosol composition with aging inferred from aerosol mass spectra, Atmos. Chem. Phys., 11, 6465–6474, doi:10.5194/acp-11-6465-2011, 2011a.

Ng, N. L., Canagaratna, M. R., Jimenez, J. L., Zhang, Q., Ulbrich, I. M., and Worsnop, D. R.: Real-Time Methods for Estimating Organic Component Mass Concentrations from Aerosol Mass Spectrometer Data, Environ. Sci. Technol., 45, 910–916, doi:10.1021/es102951k, 2011b.

Nguyen, T. B., Coggon, M. M., Bates, K. H., Zhang, X., Schwantes, R. H., Schilling, K. A., Loza, C. L., Flagan, R. C., Wennberg, P. O., and Seinfeld, J. H.: Organic aerosol formation from the reactive uptake of isoprene epoxydiols (IEPOX) onto non-acidified inorganic seeds, Atmos. Chem. Phys., 14, 3497–3510, doi:10.5194/acp-14-3497-2014, 2014.

Nguyen, T. B., Crounse, J. D., Teng, A. P., St. Clair, J. M., Paulot, F., Wolfe, G. M., and Wennberg, P. O.: Rapid deposition of oxidized biogenic compounds to a temperate forest, P. Natl. Acad. Sci., 112, E392–E401, doi:10.1073/pnas.1418702112, 2015.

Ortega, A. M., Day, D. A., Cubison, M. J., Brune, W. H., Bon, D., de Gouw, J. A., and Jimenez, J. L.: Secondary organic aerosol formation and primary organic aerosol oxidation from biomass-burning smoke in a flow reactor during FLAME-3, Atmos. Chem. Phys., 13, 11551–11571, doi:10.5194/acp-13-11551-2013, 2013.

Ortega, J., Turnipseed, A., Guenther, A. B., Karl, T. G., Day, D. A., Gochis, D., Huffman, J. A., Prenni, A. J., Levin, E. J. T., Kreidenweis, S. M., DeMott, P. J., Tobo, Y., Patton, E. G., Hodzic, A., Cui, Y. Y., Harley, P. C., Hornbrook, R. S., Apel, E. C., Monson, R. K., Eller, A. S. D., Greenberg, J. P., Barth, M. C., Campuzano-Jost, P., Palm, B. B., Jimenez, J. L., Aiken, A. C., Dubey, M. K., Geron, C., Offenberg, J., Ryan, M. G., Fornwalt, P. J., Pryor, S. C., Keutsch, F. N., DiGangi, J. P., Chan, A. W. H., Goldstein, A. H., Wolfe, G. M., Kim, S., Kaser, L., Schnitzhofer, R., Hansel, A., Cantrell, C. A., Mauldin, R. L., and Smith, J. N.: Overview of the Manitou Experimental Forest Observatory: site description and selected science results from 2008 to 2013, Atmos. Chem. Phys., 14, 6345–6367, doi:10.5194/acp-14-6345-2014, 2014.

Paulot, F., Crounse, J. D., Kjaergaard, H. G., Kroll, J. H., Seinfeld, J. H., and Wennberg, P. O.: Isoprene photooxidation: new insights into the production of acids and organic nitrates, Atmos. Chem. Phys., 9, 1479–1501, doi:10.5194/acp-9-1479-2009, 2009a.

Paulot, F., Crounse, J. D., Kjaergaard, H. G., Kürten, A., St. Clair, J. M., Seinfeld, J. H., and Wennberg, P. O.: Unexpected Epoxide Formation in the Gas-Phase Photooxidation of Isoprene, Science, 325, 730–733, doi:10.1126/science.1172910, 2009b.

Phinney, L., Leaitch, W. R., Lohmann, U., Boudries, H., Worsnop, D. R., Jayne, J. T., Toom-Sauntry, D., Wadleigh, M., Sharma, S., and Shantz, N.: Characterization of the aerosol over the subarctic north east Pacific Ocean, Deep-Sea Res. Pt. II, 53, 2410–2433, doi:10.1016/j.dsr2.2006.05.044, 2006.

Pye, H. O. T., Pinder, R. W., Piletic, I. R., Xie, Y., Capps, S. L., Lin, Y.-H., Surratt, J. D., Zhang, Z., Gold, A., Luecken, D. J., Hutzell, W. T., Jaoui, M., Offenberg, J. H., Kleindienst, T. E., Lewandowski, M., and Edney, E. O.: Epoxide Pathways Improve Model Predictions of Isoprene Markers and Reveal Key Role of Acidity in Aerosol Formation, Environ. Sci. Technol., 47, 11056–11064, doi:10.1021/es402106h, 2013.

Robinson, N. H., Hamilton, J. F., Allan, J. D., Langford, B., Oram, D. E., Chen, Q., Docherty, K., Farmer, D. K., Jimenez, J. L., Ward, M. W., Hewitt, C. N., Barley, M. H., Jenkin, M. E., Rickard, A. R., Martin, S. T., McFiggans, G., and Coe, H.: Evidence for a significant proportion of Secondary Organic Aerosol from isoprene above a maritime tropical forest, Atmos. Chem. Phys., 11, 1039–1050, doi:10.5194/acp-11-1039-2011, 2011.

Saarikoski, S., Carbone, S., Decesari, S., Giulianelli, L., Angelini, F., Canagaratna, M., Ng, N. L., Trimborn, A., Facchini, M. C., Fuzzi, S., Hillamo, R., and Worsnop, D.: Chemical characterization of springtime submicrometer aerosol in Po Valley, Italy, Atmos. Chem. Phys., 12, 8401–8421, doi:10.5194/acp-12-8401-2012, 2012.

Sage, A. M., Weitkamp, E. A., Robinson, A. L., and Donahue, N. M.: Evolving mass spectra of the oxidized component of organic aerosol: results from aerosol mass spectrometer analyses of aged diesel emissions, Atmos. Chem. Phys., 8, 1139–1152, doi:10.5194/acp-8-1139-2008, 2008.

Schneider, J., Weimer, S., Drewnick, F., Borrmann, S., Helas, G., Gwaze, P., Schmid, O., Andreae, M. O., and Kirchner, U.: Mass spectrometric analysis and aerodynamic properties of various types of combustion-related aerosol particles, Int. J. Mass. Spectrom., 258, 37–49, doi:10.1016/j.ijms.2006.07.008, 2006.

Schneider, J., Freutel, F., Zorn, S. R., Chen, Q., Farmer, D. K., Jimenez, J. L., Martin, S. T., Artaxo, P., Wiedensohler, A., and Borrmann, S.: Mass-spectrometric identification of primary biological particle markers and application to pristine submicron aerosol measurements in Amazonia, Atmos. Chem. Phys., 11, 11415–11429, doi:10.5194/acp-11-11415-2011, 2011.

Setyan, A., Zhang, Q., Merkel, M., Knighton, W. B., Sun, Y., Song, C., Shilling, J. E., Onasch, T. B., Herndon, S. C., Worsnop, D. R., Fast, J. D., Zaveri, R. A., Berg, L. K., Wiedensohler, A., Flowers, B. A., Dubey, M. K., and Subramanian, R.: Characterization of submicron particles influenced by mixed biogenic and anthropogenic emissions using high-resolution aerosol mass spectrometry: results from CARES, Atmos. Chem. Phys., 12, 8131–8156, doi:10.5194/acp-12-8131-2012, 2012.

Slowik, J. G., Brook, J., Chang, R. Y.-W., Evans, G. J., Hayden, K., Jeong, C.-H., Li, S.-M., Liggio, J., Liu, P. S. K., McGuire, M., Mihele, C., Sjostedt, S., Vlasenko, A., and Abbatt, J. P. D.: Photochemical processing of organic aerosol at nearby continental sites: contrast between urban plumes and regional aerosol, Atmos. Chem. Phys., 11, 2991–3006, doi:10.5194/acp-11-2991-2011, 2011.

Surratt, J. D., Kroll, J. H., Kleindienst, T. E., Edney, E. O., Claeys, M., Sorooshian, A., Ng, N. L., Offenberg, J. H., Lewandowski, M., Jaoui, M., Flagan, R. C., and Seinfeld, J. H.: Evidence for organosulfates in secondary organic aerosol, Environ. Sci. Technol., 41, 517–527, doi:10.1021/Es062081q, 2007.

Surratt, J. D., Chan, A. W. H., Eddingsaas, N. C., Chan, M., Loza, C. L., Kwan, A. J., Hersey, S. P., Flagan, R. C., Wennberg, P. O., and Seinfeld, J. H.: Reactive intermediates revealed in secondary organic aerosol formation from isoprene, P. Natl. Acad. Sci., 107, 6640–6645, doi:10.1073/pnas.0911114107, 2010.

Takegawa, N., Miyakawa, T., Kawamura, K., and Kondo, Y.: Contribution of selected dicarboxylic and omega-oxocarboxylic acids in ambient aerosol to the $m/z$ 44 signal of an aerodyne aerosol mass spectrometer, Aerosol. Sci. Tech., 41, 418–437, doi:10.1080/02786820701203215, 2007.

Ulbrich, I. M., Canagaratna, M. R., Zhang, Q., Worsnop, D. R., and Jimenez, J. L.: Interpretation of organic components from Positive Matrix Factorization of aerosol mass spectrometric data, Atmos. Chem. Phys., 9, 2891–2918, doi:10.5194/acp-9-2891-2009, 2009.

Wang, W., Kourtchev, I., Graham, B., Cafmeyer, J., Maenhaut, W., and Claeys, M.: Characterization of oxygenated derivatives of isoprene related to 2-methyltetrols in Amazonian aerosols using trimethylsilylation and gas chromatography/ion trap mass spectrometry, Rapid Commun. Mass. Sp., 19, 1343–1351, doi:10.1002/rcm.1940, 2005.

Weimer, S., Alfarra, M. R., Schreiber, D., Mohr, M., Prévôt, A. S. H., and Baltensperger, U.: Organic aerosol mass spectral signatures from wood-burning emissions: Influence of burning conditions and wood type, J. Geophys. Res., 113, D10304, doi:10.1029/2007jd009309, 2008.

Worton, D. R., Surratt, J. D., LaFranchi, B. W., Chan, A. W. H., Zhao, Y., Weber, R. J., Park, J.-H., Gilman, J. B., de Gouw, J., Park, C., Schade, G., Beaver, M., Clair, J. M. S., Crounse, J., Wennberg, P., Wolfe, G. M., Harrold, S., Thornton, J. A., Farmer, D. K., Docherty, K. S., Cubison, M. J., Jimenez, J.-L., Frossard, A. A., Russell, L. M., Kristensen, K., Glasius, M., Mao, J., Ren, X., Brune, W., Browne, E. C., Pusede, S. E., Cohen, R. C., Seinfeld, J. H., and Goldstein, A. H.: Observational Insights into Aerosol Formation from Isoprene, Environ. Sci. Technol., 47, 11403–11413, doi:10.1021/es4011064, 2013.

Xu, L., Guo, H., Boyd, C. M., Klein, M., Bougiatioti, A., Cerully, K. M., Hite, J. R., Isaacman-VanWertz, G., Kreisberg, N. M., Knote, C., Olson, K., Koss, A., Goldstein, A. H., Hering, S. V., de Gouw, J., Baumann, K., Lee, S.-H., Nenes, A., Weber, R. J., and Ng, N. L.: Effects of anthropogenic emissions on aerosol formation from isoprene and monoterpenes in the southeastern United States, P. Natl. Acad. Sci., 112, 37–42, doi:10.1073/pnas.1417609112, 2014.

Xu, L., Suresh, S., Guo, H., Weber, R. J., and Ng, N. L.: Aerosol characterization over the southeastern United States using high-resolution aerosol mass spectrometry: spatial and seasonal variation of aerosol composition and sources with a focus on organic nitrates, Atmos. Chem. Phys., 15, 7307–7336, doi:10.5194/acp-15-7307-2015, 2015.

Zhang, H., Worton, D. R., Lewandowski, M., Ortega, J., Rubitschun, C. L., Park, J.-H., Kristensen, K., Campuzano-Jost, P., Day, D. A., Jimenez, J. L., Jaoui, M., Offenberg, J. H., Kleindienst, T. E., Gilman, J., Kuster, W. C., de Gouw, J., Park, C., Schade, G. W., Frossard, A. A., Russell, L., Kaser, L., Jud, W., Hansel, A., Cappellin, L., Karl, T., Glasius, M., Guenther, A., Goldstein, A. H., Seinfeld, J. H., Gold, A., Kamens, R. M., and Surratt, J. D.: Organosulfates as Tracers for Secondary Organic Aerosol (SOA) Formation from 2-Methyl-3-Buten-2-ol (MBO) in the Atmosphere, Environ. Sci. Technol., 46, 9437–9446, doi:10.1021/es301648z, 2012.

Zhang, H., Zhang, Z., Cui, T., Lin, Y.-H., Bhathela, N. A., Ortega, J., Worton, D. R., Goldstein, A. H., Guenther, A., Jimenez, J. L., Gold, A., and Surratt, J. D.: Secondary Organic Aerosol Formation via 2-Methyl-3-buten-2-ol Photooxidation: Evidence of Acid-Catalyzed Reactive Uptake of Epoxides, Environ. Sci. Technol. Lett., 1, 242–247, doi:10.1021/ez500055f, 2014.